ChemCatChem

Supporting Information

# Tailored Coumarin Dyes for Photoredox Catalysis: Calculation, Synthesis, and Electronic Properties

Andrea Gualandi[+],* Artur Nenov[+],* Marianna Marchini, Giacomo Rodeghiero, Irene Conti, Ettore Paltanin, Matteo Balletti, Paola Ceroni,* Marco Garavelli,* and Pier Giorgio Cozzi*

# SUPPORTING INFORMATION

**Table of Contents**

# 1. **Experimental Procedures**

## 1.1. General methods and materials

$^{1}$H-NMR spectra were recorded on Varian Mercury 400 spectrometer. Chemical shifts are reported in ppm from TMS with the solvent resonance as the internal standard ($CDCl_3$: δ = 7.27 ppm). Data are reported as follows: chemical shift, multiplicity (s = singlet, d = duplet, t = triplet, q = quartet, dd = double duplet, dt = double triplet, bs = broad signal, m = multiplet), coupling constants (Hz). $^{13}$C-NMR spectra were recorded on Varian MR400 spectrometer with $^{1}$H fully decoupled. Chemical shifts are reported in ppm from TMS with the solvent as the internal standard ($CDCl_3$: δ = 77.0 ppm). GC-MS spectra were taken by EI ionization at 70 eV on a Hewlett-Packard 5971 with GC injection. LC-electrospray ionization mass spectra (ESI-MS) were obtained with Agilent Technologies MSD1100 single-quadrupole mass spectrometer. HRMS were performed on Waters Xevo G2-XS QTof, ESI+, cone voltage 40 V, Capillary 3KV, source temperature 120 °C.
Chromatographic purification was done with 240-400 mesh silica gel. All reactions were set up under an argon atmosphere in oven-dried glassware using standard Schlenk techniques.
Anhydrous solvents were supplied by Aldrich in Sureseal® bottles and were used without further purification. All the reagents were purchased from Aldrich and used without further purification unless specified. Triethylamine and DIPEA were stirred one day over KOH and distilled before their use.
Coumarines **1**,[1] **2**,[1] **5**[2] were prepared according to the procedure reported in literature.

**Figure S1.** Emission profile of the 16W Blue LED strip used to irradiate the solutions.

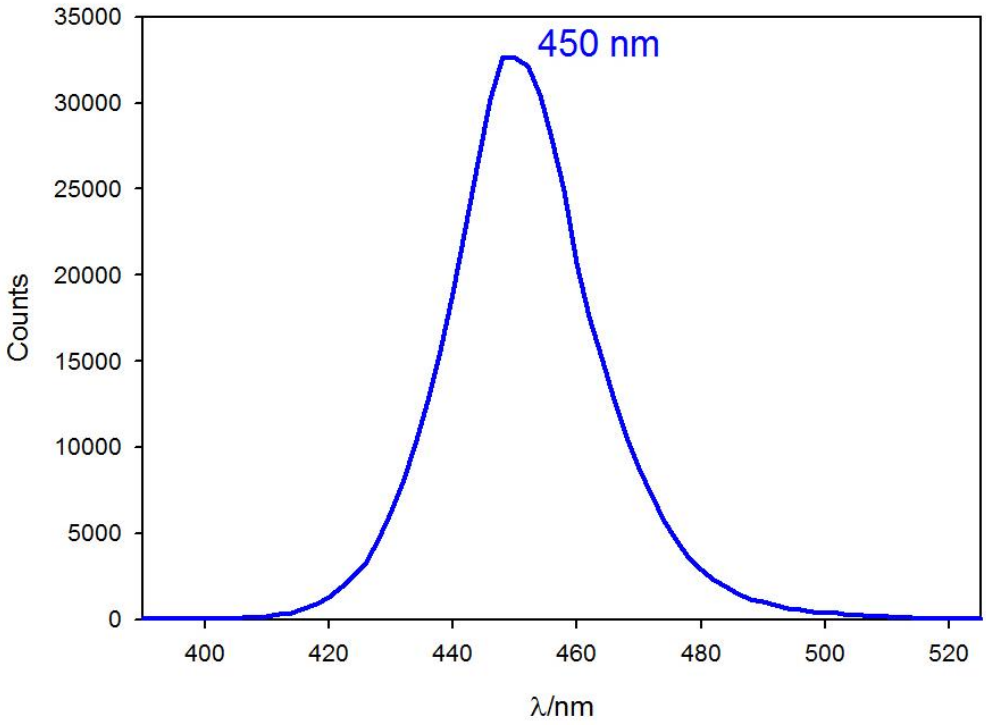

**1.2 Synthesis and characterization of coumarins**

*1.2.1 Synthesis of boronic acid*

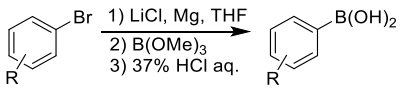


4-(dimethylamino)phenylboronic acid was prepared according to reported procedure[3]: to anhydrous LiCl under inert atmosphere, THF (2 mL), magnesium turnings (4.5 mmol, 100 mg) and DIBALH (1M in THF, 0.02 mmol) were added. A solution of 4-bromo-*N*,*N*-dimethylaniline (1.75 mmol, 350 mg) in THF (4 mL) was added dropwise to the mixture, and the reaction was stirred for 1 hours. The solution was cooled at 0°C, $B(OMe)_3$ (3.5 mmol, 364 mg, 0.391 mL) was added and the solution was stirred for 1 hour. 37% HCl aq. was slowly added until pH = 4 and the solution was stirred for 30 minutes. The mixture was extracted with AcOEt (3 x 10 mL), the organic phases were dried over $Na_2SO_4$, and the solvent was removed under reduced pressure to obtain 4-(dimethylamino)benzene boronic acid as white solid (57%, 1.0 mmol, 0.166 g); Spectroscopic properties correspond to the literature.[3]

3,5-dimethoxy-phenylboronic acid was prepared using the same procedure reported for 4-(dimethylamino)phenylboronic acid on 3,5-dimethoxy-bromobenzene to obtain 4-(dimethylamino)benzene boronic acid as white solid (73%, 1.27 mmol, 0.233 g); Spectroscopic properties correspond to the literature.[4]

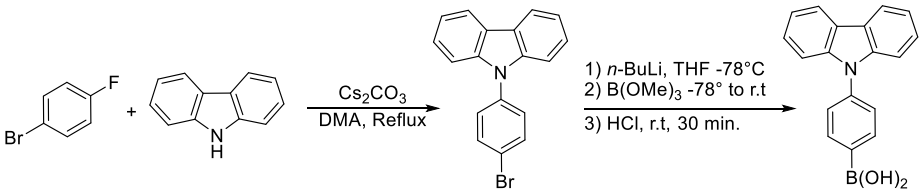


*N*-(4-bromophenyl)carbazole was prepared according to reported procedure:[5] A mixture of 4-bromo-fluorobenzene (3.6 mmol, 393 μl), carbazole (0.6 mmol, 300 mg), anhydrous DMA (10 mL) and $Cs_2CO_3$ (10.5 mmol, 3,6 g) was refluxed until under inert atmosphere disappear of the carbazole (about 20 hours by TLC analysis). The reaction mixture was cooled at room temperature, water (25 mL) and diethyl ether (20 mL) were added. The two phases were separated, and water phase was extracted with diethyl ether (2 x 20 mL). The organic phases were dried over $Na_2SO_4$, and the solvent was removed under reduced pressure to obtain sticky solid. Pure compound was obtained after chromatographic purification ($SiO_2$, cyclohexane:ethyl acetate 95:5) to give desired product (56%, 1.02 mmol, 0.324 g) as brownish solid; Spectroscopic properties correspond to the literature.[5]

4-(carbazol-9-yl)phenylboronic acid was prepared according to reported procedure:[6] To a stirred solution of *N*-(4-bromophenyl)carbazole (0.93 mmol, 300 mg) in anhydrous THF (10 ml) at -78 °C a solution of *n*-BuLi (2.5 M in hexanes, 1.4 mmol, 0.56 mL). The reaction was stirred at -78 °C for 1.5 hours and $B(OMe)_3$ (1.86 mmol, 208 μl) was slowly added. The mixture was warmed at room temperature and stirred for 2 hours. HCl (37% acq., 7 mL) was slowly added and the mixture was stirred for 30 minutes. AcOEt (10 mL) was added, the two phases were separated, and water phase was extracted with AcOEt (2 x 10 mL). The organic phases were dried over $Na_2SO_4$, and the solvent was removed under reduced pressure to obtain white solid. The solid was washed with small portion of diethyl ether to obtain pure product (47%, 0.44 mmol, 0.125 g) as white solid; Spectroscopic properties correspond to the literature.[7]

*1.2.2 Synthesis of 3-bromo-7-diethylaminocoumarin (**14**)*

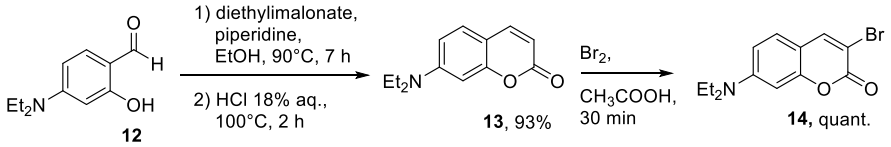


7-diethylaminocoumarin (**13**) and 3-bromo-7-diethylaminocoumarin (**14**) were prepared according to literature procedure.[8]

(**13**): In a two necks round bottom flask under inert atmosphere were added 4-diethylamino salycilaldehyde (10 mmol, 2.2 g), absolute ethanol (20 mL), diethylmalonate (20 mmol, 3.2 g, 3.1 mL) and piperidine (1 mmol, 0.085 g, 99 μL). The solution was refluxed for 7 hours until disappearance of aldehyde, cooled at room temperature and the solvent was removed under reduced pressure. The residue was dissolved in DCM (20 mL), washed with 2 M HCl aq. (2 x 10 mL) and brine (2 x 10 mL). The organic phase was evaporated, the residue was suspended in 18% HCl aq. and refluxed for 2 hours. The solution was cooled at room temperature and 4M NaOH aq. was added until neutral pH. DCM (20 mL) was added and the two phases separated. The organic phase was washed with brine (2x 5 mL), dried over $Na_2SO_4$, and the solvent was removed under reduced pressure to obtain 7-diethylaminocoumarin as red solid (93%, 9.3 mmol, 2.02 g); $^1$H-NMR (400 MHz, $CDCl_3$) δ: 7.50 (d, *J* = 9.3 Hz, 1H), 7.23 (d, *J* = 8.5 Hz, 1H), 6.53 (dd, *J* = 8.8, 2.4 Hz, 1H), 6.45 (d,

*J* = 2.2 Hz, 1H), 6.00 (d, *J* = 9.3 Hz, 1H), 3.38 (q, *J* = 7.1 Hz, 4H), 1.18 (t, *J* = 7.1 Hz, 6H). Spectroscopic properties correspond to the literature.[8]

(**14**): To a solution of 7-diethylaminocoumarin (4.6 mmol, 0.998 g) in glacial acetic acid (10 mL) a solution of bromine (4.6 mmol, 0.735 g, 0.236 mL) in glacial acetic acid (5 mL) was added dropwise under stirring. After 30 minutes the solid was filtered and washed with water (3 x 10 mL) and dried under vacuum to give 3-bromo-7-diethylaminocoumarin in quantitative yield as orange solid; Spectroscopic properties correspond to the literature.[8]

*1.2.3 Synthesis of **6**, **7**, **9**, **10**, **11** by Suzuki-Miyaura coupling*

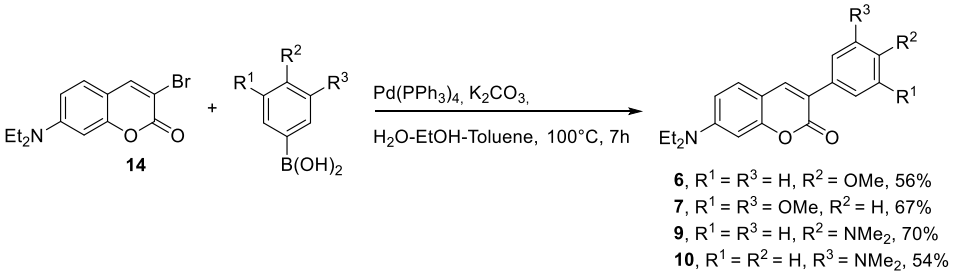


**6**, $R^1 = R^3 = H$, $R^2 = OMe$, 56%
**7**, $R^1 = R^3 = OMe$, $R^2 = H$, 67%
**9**, $R^1 = R^3 = H$, $R^2 = NMe_2$, 70%
**10**, $R^1 = R^2 = H$, $R^3 = NMe_2$, 54%

(**6**): To a degassed mixture of water:ethanol:toluene (10:5:5 mL) under inert atmosphere 3-bromo-7-diethylaminocoumarin (0.17 mmol, 0.050 g), $Pd(PPh_3)_4$ (0.008 mmol, 9.2 mg), 4-(dimethylamino) benzene boronic acid (0.34 mmol, 0.056 g) e $K_2CO_3$ (0.51 mmol, 0.070 g) were added. The mixture was refluxed for 7 hours, cooled at room temperature and the solvents were evaporated under reduced pressure. The reside was diluted with DCM (40 mL) and filtered through Celite®. The solvent was evaporated under reduced pressure and the residue was purified by flash chromatography ($SiO_2$, cyclohexane:ethyl acetate 95:5) to give **6** (0.11 mmol, 0.037 g) as red solid; $^1$H-NMR (400 MHz, $CDCl_3$) δ: 7.69 – 7.58 (m, 3H), 7.27 (d, *J* = 8.8 Hz, 1H), 6.98 – 6.88 (m, 2H), 6.57 (dd, *J* = 8.7, 2.4 Hz, 1H), 6.51 (d, *J* = 2.3 Hz, 1H), 3.81 (s, 3H), 3.40 (q, *J* = 7.1 Hz, 4H), 1.19 (t, *J* = 7.1 Hz, 6H); $^{13}$C{$^1$H}-NMR (400 MHz, $CDCl_3$) δ: 161.8, 159.2, 155.9, 150.2, 139.4, 129.4 (2C), 128.7, 128.2, 120.6, 113.7 (2C), 109.2, 108.9, 97.1, 55.3, 44.8, 12.4; ESI-MS *m/z*: 324.2 $[M + H]^+$; HRMS (ESI/Flow Injection): Calcd for $C_{20}H_{22}NO_3$ $[M+H]^+$ 324.15942; Found 324.15928.

(**7**): The general procedure reported for **6** was applied; yield 56% (0.10 mmol, 0.034 g); red solid; $^1$H-NMR (400 MHz, $CDCl_3$) δ: 7.68 (s, 1H), 7.29 (d, *J* = 8.8 Hz, 1H), 6.84 (d, *J* = 2.2 Hz, 2H), 6.58 (dd, *J* = 8.8, 2.4 Hz, 1H), 6.51 (d, *J* = 2.2 Hz, 1H), 6.44 (t, *J* = 2.2 Hz, 1H), 3.81 (s, 6H), 3.41 (q, *J* = 7.1 Hz, 4H), 1.20 (t, *J* = 7.1 Hz, 6H); $^{13}$C{$^1$H}-NMR (400 MHz, $CDCl_3$) δ: 161.4, 160.5 (2C), 156.2, 150.5, 140.7, 137.7, 129.0 (2C), 120.6, 108.9, 106.4 (2C), 100.1, 97.0, 55.4 (2C), 44.8 (2C), 12.4 (2C); ESI-MS *m/z*: 354.2 $[M + H]^+$; HRMS (ESI/Flow Injection): Calcd for $C_{21}H_{23}NO_4$ $[M+H]^+$ 354.16998; Found 354.16970.

(**9**): The general procedure reported for **6** was applied; yield 70% (0.12 mmol, 0.040 g); yellow solid; $^1$H-NMR (400 MHz, $CDCl_3$) δ: 7.63 (m, 3H), 7.30 (d, *J* = 8.8 Hz, 1H), 6.78 (d, *J* = 8.8 Hz, 2H), 6.59 (dd, *J* = 8.7, 2.2 Hz, 1H), 6.54 (d, *J* = 2.0 Hz, 1H), 3.43 (q, *J* = 7.1 Hz, 4H), 2.99 (s, 6H), 1.22 (t, *J* = 7.1 Hz, 6H); $^{13}$C{$^1$H}-NMR (400 MHz, $CDCl_3$) δ: 162.0, 155.6, 150.1, 149.8, 137.9, 128.9 (2C), 128.4, 123.7, 121.2, 112.2 (2C), 109.5, 108.7, 97.2, 44.8 (2C), 40.5 (2C), 12.5 (2C); ESI-MS *m/z*: 337.2 $[M+H]^+$; HRMS (ESI/Flow Injection): Calcd for $C_{21}H_{25}N_2O_2$ $[M+H]^+$ 337.19105; Found 337.19079.

(**10**): The general procedure reported for **6** was applied; yield 54% (0.09 mmol, 0.031 g); yellow solid; $^1$H-NMR (400 MHz, $CDCl_3$) δ: 7.67 (s, 1H), 7.28 (t, *J* = 8.2 Hz, 2H), 7.05 (s, 1H), 6.99 (d, *J* = 7.6 Hz, 1H), 6.72 (dd, *J* = 8.3, 2.1 Hz, 1H), 6.57 (dd, *J* = 8.8, 2.4 Hz, 1H), 6.51 (d, *J* = 2.2 Hz, 1H), 3.41 (q, *J* = 7.1 Hz, 4H), 2.97 (s, 6H), 1.20 (t, *J* = 7.1 Hz, 6H); $^{13}$C{$^1$H}-NMR (400 MHz, $CDCl_3$) δ: 161.6, 156.1, 150.6, 150.3, 140.3, 136.5, 128.9, 128.8, 121.8, 116.8, 112.8, 112.3, 109.1, 108.8, 97.1, 77.3, 77.0, 76.7, 44.8, 40.7, 12.4; ESI-MS *m/z*: 337.2 $[M + H]^+$; 673.4 $[1M + H]^+$; HRMS (ESI/Flow Injection): Calcd for $C_{21}H_{25}N_2O_2$ $[M+H]^+$ 337.19105; Found 337.19061.

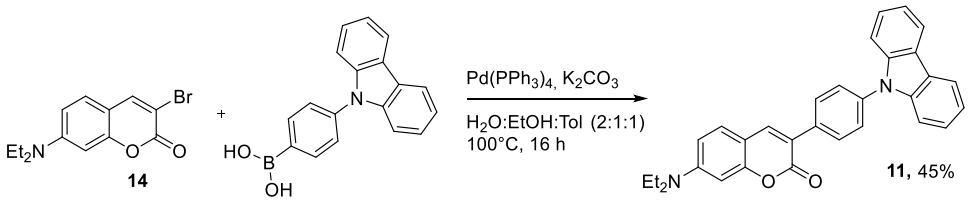


**11**, 45%

(**11**): The general procedure reported for **6** was applied but with a reaction time of 16 hours; yield 45% (0.07 mmol, 0.035 g); yellow solid; $^1$H NMR (400 MHz, $CDCl_3$) δ: 8.14 (d, *J* = 7.7 Hz, 2H), 7.94 (d, *J* = 8.3 Hz, 2H), 7.81 (s, 1H), 7.60 (d, *J* = 8.3 Hz, 2H), 7.47 (d, *J* = 8.3 Hz, 2H), 7.41 (t, *J* = 7.6 Hz, 2H), 7.35 (d, *J* = 8.7 Hz, 1H), 7.28 (t, *J* = 7.4 Hz, 2H), 6.62 (dd, *J* = 8.9, 2.1 Hz, 1H), 6.57 (s, 1H), 3.44 (q, *J* = 7.2 Hz, 4H), 1.23 (t, *J* = 7.0 Hz, 6H); $^{13}$C{$^1$H}-NMR (400 MHz, $CDCl_3$) δ: 161.7, 156.3, 150.7, 140.8, 140.8, 134.9, 129.6

(2C), 129.1, 126.8 (2C), 125.9 (2C), 123.4, 120.3 (2C), 119.9 (2C), 119.8, 109.9 (2C), 109.1, 109.1, 97.1, 44.9, 12.5.; ESI-MS m/z: 459.2 $[M + H]^+$; HRMS (ESI/Flow Injection): Calcd for $C_{31}H_{27}N_2O_2$ $[M+H]^+$ 459.20670; Found 459.20666.

*1.2.4 Synthesis of **3***

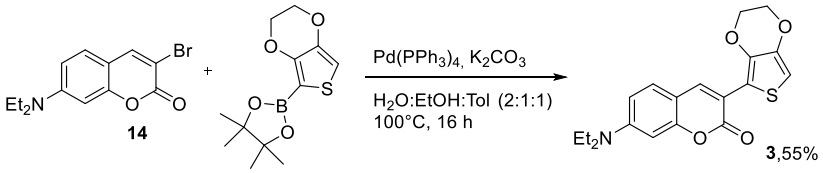


The general procedure reported for **6** was applied but using pinacol arylboronate instead of arylboronic acid; yield 55% (0.09 mmol, 0.033 g); green solid; $^1$H-NMR (400 MHz, $CDCl_3$) δ: 8.42 (s, 1H), 7.30 (d, *J* = 8.8 Hz, 1H), 6.59 (dd, *J* = 8.9, 2.4 Hz, 1H), 6.51 (d, *J* = 2.1 Hz, 1H), 6.39 (s, 1H), 4.39 – 4.31 (m, 2H), 4.28 – 4.19 (m, 2H), 3.41 (q, *J* = 6.9 Hz, 4H), 1.20 (t, *J* = 7.1 Hz, 6H); $^{13}$C{$^1$H}-NMR (400 MHz, $CD_2Cl_2$) δ: 157.4, 155.3, 150.9, 144.2, 137.5, 129.4, 129.3, 109.8, 109.5, 109.2, 100.7, 97.9, 97.5, 65.6, 65.0, 45.4, 45.3, 12.8, 12.7; ESI-MS *m/z*: 358.2 $[M + H]^+$; HRMS (ESI/Flow Injection): Calcd for $C_{20}H_{22}NO_3$ $[M+H]^+$ 358.11076; Found 358.11054.

*1.2.5 Synthesis of **4***

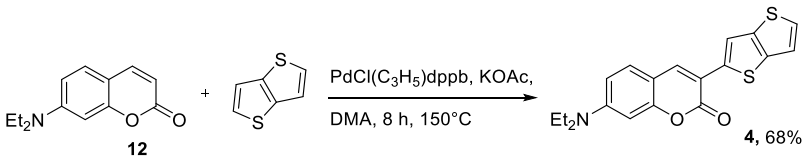


Compound **4** was prepared according to reported procedure.[9] Thieno[3,2-*b*]thiophene (0.5 mmol, 70 mg), KOAc (0.5 mmol, 49 mg), 3-bromo-7-diethylaminocoumarin (0.25 mmol, 74 mg), and palladium complex (0.0025 mmol, 1.5 mg)[10] were dissolved in degassed DMA (6 mL). The mixture was refluxed for 8 hours, cooled at room temperature. Water (5 mL) and AcOEt (20 mL) were added to the mixture. The two phases were separated, and water phase was extracted with AcOEt (2 x 10 mL). The organic phases were dried over $Na_2SO_4$, and the solvent was removed under reduced pressure to obtain orange solid. Pure compound was obtained after chromatographic purification ($SiO_2$, cyclohexane:ethyl acetate 85:15) to give **4** (68%, 0.17 mmol, 0.060 g) as yellow solid; $^1$H-NMR (400 MHz, $CDCl_3$) δ: 7.96 (s, 1H), 7.84 (s, 1H), 7.37 – 7.29 (m, 2H), 7.22 (d, *J* = 5.2 Hz, 1H), 6.60 (d, *J* = 8.9 Hz, 1H), 6.52 (s, 1H), 3.42 (q, *J* = 7.0 Hz, 4H), 1.21 (t, *J* = 7.2 Hz, 6H).; $^{13}$C{$^1$H}-NMR (400 MHz, $CDCl_3$) δ: 160.1, 155.5, 150.6, 139.9, 139.8, 138.7, 136.8, 128.9, 127.3, 119.4, 117.9, 114.9, 109.3, 108.7, 97.1, 44.9 (2C), 12.5 (2C); ESI-MS *m/z*: 356.0 $[M + H]^+$; HRMS (ESI/Flow Injection): Calcd for $C_{19}H_{18}NO_2S_2$ $[M+H]^+$ 356.07735; Found 356.07721.

*1.2.6 Synthesis of **8***

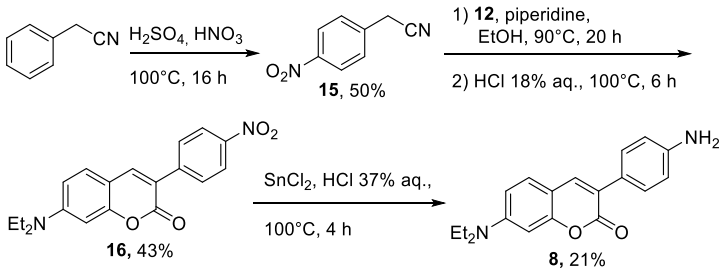

**8** was prepared according to reported procedure:[11] 4-diethylamino-salicyl aldehyde (1.2 mmol, 0.232 g) was dissolved in absolute ethanol (7 mL) under inert atmosphere. 2-(4-nitrophenyl)acetonitrile (1.2 mmol, 0.200 g), prepared according to reported procedure,[12] was added to the solution followed by 5 drops of piperidine. The reaction mixture was stirred overnight, and the solvent was evaporated under reduce pressure to obtain a red solid. The solid was added to 10% HCl aq. (10 mL) and the suspension was refluxed for 6 hours. The mixture was cooled at room temperature, the result orange solid was filtered off and washed with water. The solid was purified by flash chromatography ($SiO_2$, cyclohexane:ethyl acetate 8:2) to obtain **16** as orange solid (43%, 0.516 mmol, 0.174 g); $^1$H-NMR (400 MHz, $CDCl_3$) $\delta$: 8.26 (d, *J* = 8.7 Hz, 2H), 7.92 (d, *J* = 8.7 Hz, 2H), 7.83 (s, 1H), 7.36 (d, *J* = 8.9 Hz, 1H), 6.64 (dd, *J* = 8.8, 2.3 Hz, 1H), 6.54 (d, *J* = 2.1 Hz, 1H), 3.46 (q, *J* = 7.1 Hz, 4H), 1.25 (t, *J* = 7.1 Hz, 6H); $^{13}$C{$^1$H}-NMR (400 MHz, $CDCl_3$) $\delta$: 160.9, 156.7, 151.4, 146.7, 142.5, 142.1, 129.6, 128.6 (2C), 123.5 (2C), 117.7, 109.4, 108.7, 97.0, 45.0, 12.4; ESI-MS *m/z*: 339.2 $[M+H]^+$.
In a two necks round bottom flask under air tin(II) chloride hydrate (0.9 mmol, 195 mg) was dissolvent in HCl (37% aq., 1.5 mL). Compound **16** (0.2 mmol, 0.068 g) was slowly added to the solution, the mixture was refluxed for 4 hours and cooled at room temperature. NaOH 1 M was slowly added to the mixture until neutral pH and the mixture was extracted with AcOEt (3 x 15 mL). The organic phases were washed with brine (2 x 5 mL), dried over $Na_2SO_4$, and the solvent was removed under reduced pressure to give a brown solid. The crude was further purified by flash column chromatography ($SiO_2$, cyclohexane:ethyl acetate 8:2) to obtain **8** as red solid, 61% yield (0.12 mmol, 0.038 mg); $^1$H-NMR (400 MHz, $CDCl_3$) $\delta$: 7.58 (s, 1H), 7.50 (d, *J* = 8.2 Hz, 2H), 7.26 (d, *J* = 8.9 Hz, 1H), 6.73 (d, *J* = 8.1 Hz, 2H), 6.56 (d, *J* = 8.9 Hz, 1H), 6.50 (s, 1H), 3.39 (q, *J* = 6.9 Hz, 4H), 1.19 (t, *J* = 7.0 Hz, 6H); $^{13}$C{$^1$H}-NMR (400 MHz, $CDCl_3$) $\delta$: 161.9, 155.8, 150.0, 146.2, 138.5, 129.2 (2C), 128.5, 125.9, 121.1, 114.8 (2C), 109.3, 108.8, 97.2, 44.8 (2C), 12.5 (2C); ESI-MS *m/z*: 309.1 $[M+H]^+$; HRMS (ESI/Flow Injection): Calcd for $C_{19}H_{21}N_2O_2$ $[M+Na]^+$ 331.14170; Found 331.14160.

### 1.3 General procedures for photoredox pinacol coupling of aldehydes.

**Procedure with TEA**: A dry 10 mL Schlenk tube, equipped with a Rotaflo stopcock, magnetic stirring bar and an argon supply tube, was charged in order and under argon with the coumarin photocatalyst (5 mol%, 0.01 mmol), aldehyde **17** (0.2 mmol, 0.028 g) and DMF (1.0 mL). The reaction mixture was then subjected to a freeze-pump-thaw procedure (three cycles) and the vessel refilled with argon. Then the $Et_3N$ was added (0.8 mmol, 4 equiv., 112 µL).

**Procedure with BIH and Oxalic acid**: A dry 10 mL Schlenk tube, equipped with a Rotaflo stopcock, magnetic stirring bar and an argon supply tube, was charged in order and under argon with the coumarin photocatalyst (5 mol%, 0.01 mmol), aldehyde **17** (0.2 mmol, 0.028 g), BIH (0.4 mmol, 0.078 g), oxalic acid (0.2 mmol, 0.018 g) and DMF (1.0 mL). The reaction mixture was then subjected to a freeze-pump-thaw procedure (three cycles) and the vessel refilled with argon.

The reaction was irradiated with 16W blue LEDs (approx. 10 cm distance) and stirred for 36 h. After that the reaction mixture was diluted with $H_2O$ (5 mL) extracted with AcOEt (3 x 10 mL). The combined organic layers were washed with brine (10 mL), dried over $Na_2SO_4$, and the solvent was removed under reduced pressure. The residue was purified by flash column chromatography ($SiO_2$) to afford the title compounds in the stated yields. Diastereoisomeric ratio was determined by integration of benzylic C<u>H</u> $^1$H NMR signal; $^1$H-NMR (400 MHz, $CDCl_3$, 25°C): $\delta_{d/l,meso}$ = 7.24 (*meso*, m, 4H), 7.22–7.17 (*d/l*, m, 4H), 7.11–7.06 (*meso*, m, 4H), 7.03–6.98 (*d/l*, m, 4H), 4.82 (*meso*, s, 2H), 4.60 (*d/l*, s, 2H); $^{13}$C{$^1$H}-NMR (100 MHz, $CDCl_3$): $\delta_{d/l,meso}$ = 137.9 (*meso*, 2C), 137.8 (*d/l*, 2C), 133.8 (4C), 128.4 (*meso*, 4C), 128.3 (*d/l*, 4C), 128.3 (8C), 78.5 (2C), 77.1 (2C); ESI-MS *m/z*: 265.0 $[M-OH]^+$, 305.1 $[M+Na]^+$.

## 2. Copies of NMR spectra

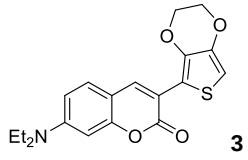


**3**

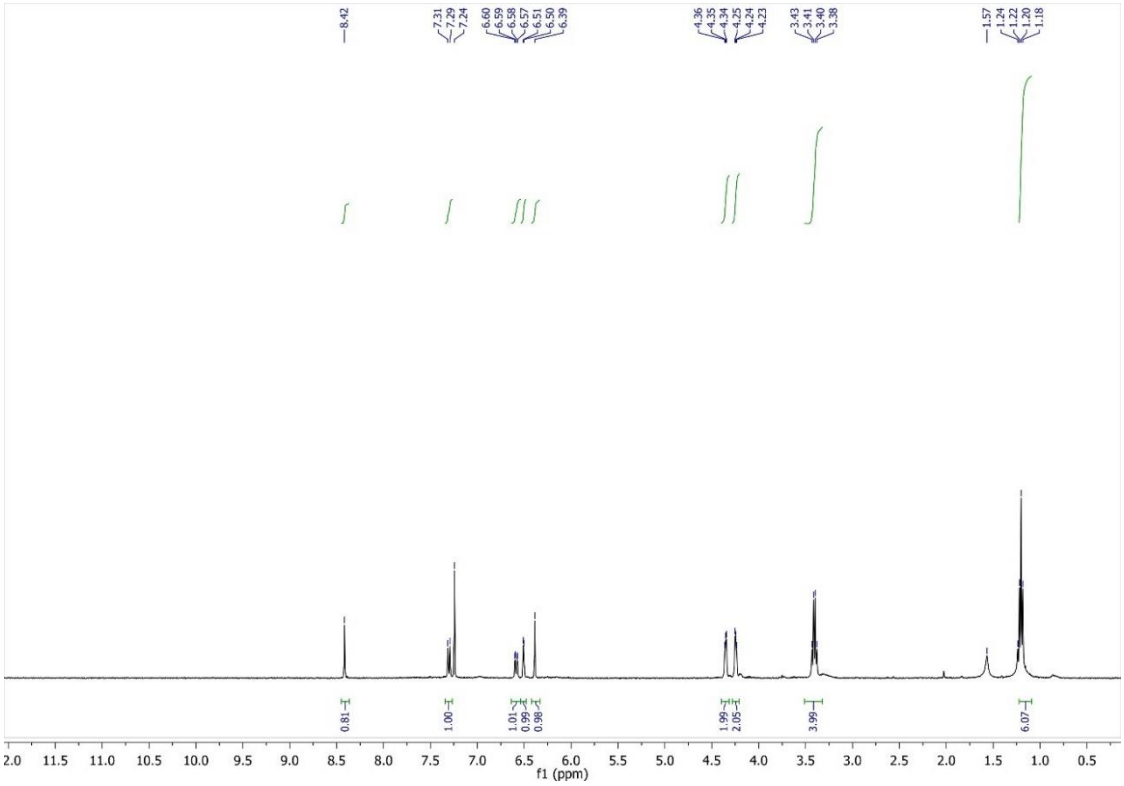


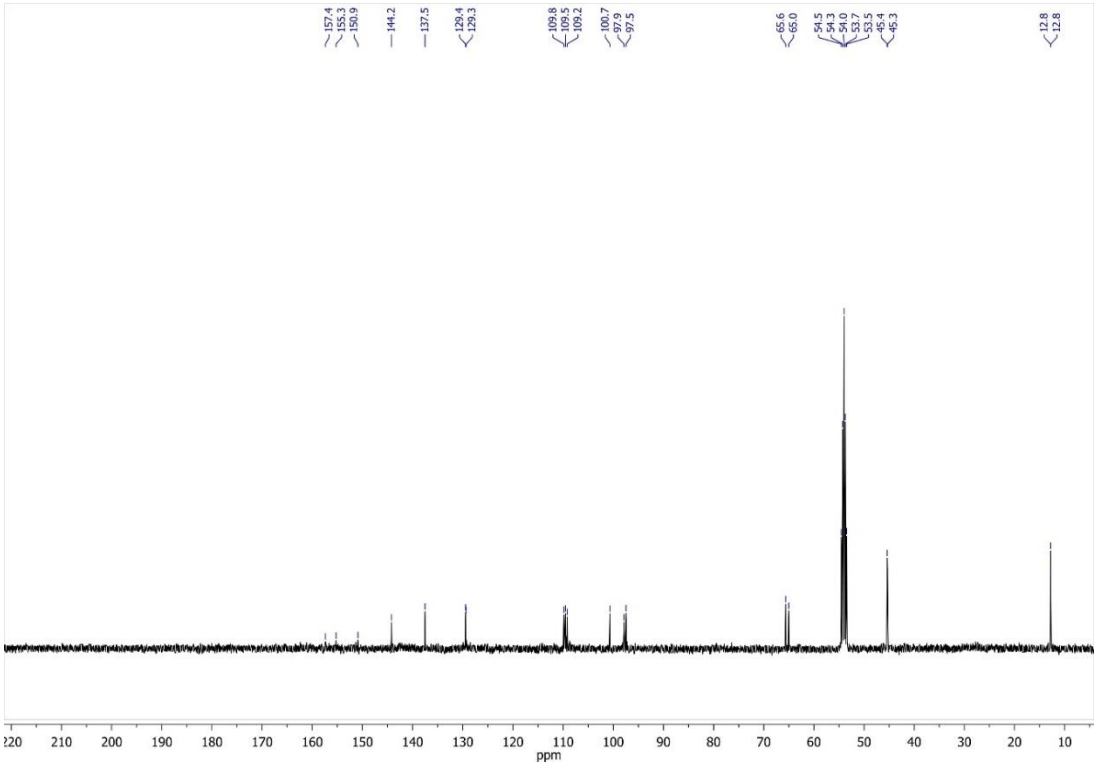

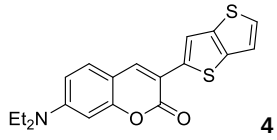
S
S
Et2N
O
O

**4**

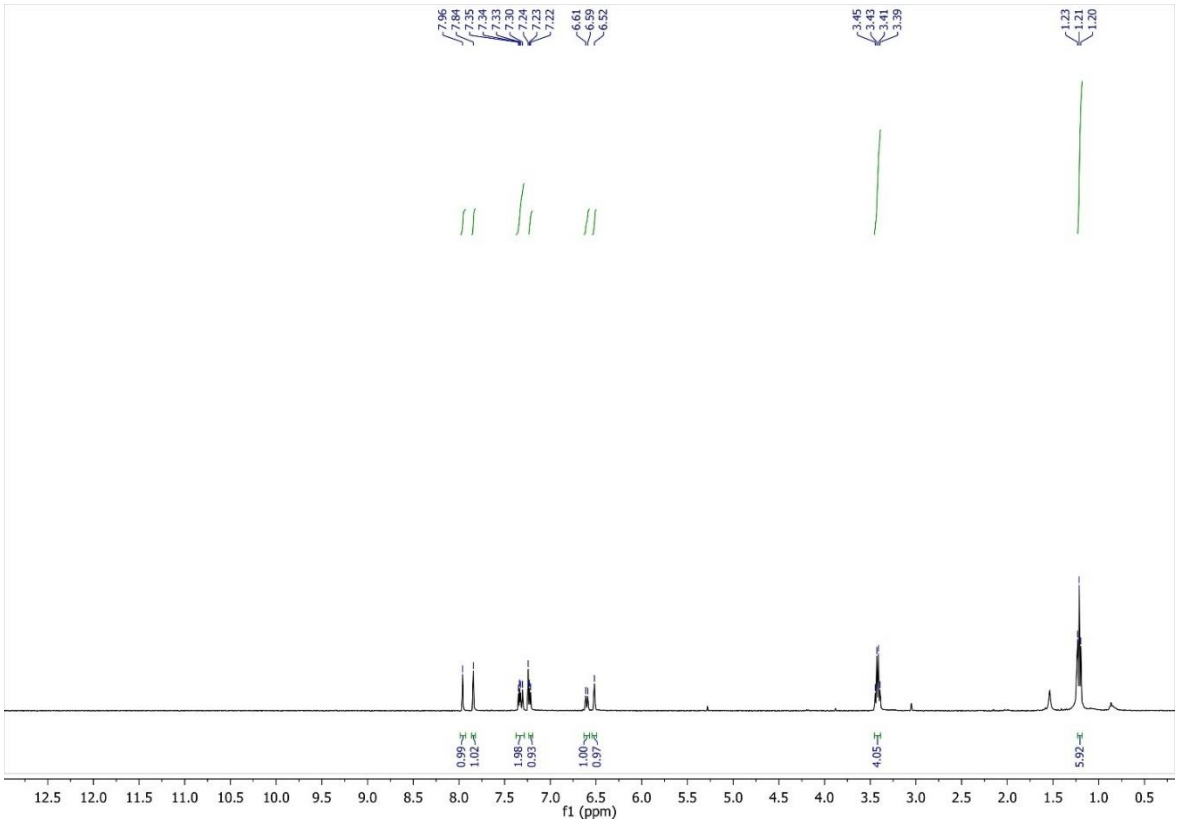
7.96
7.84
7.35
7.34
7.33
7.30
7.24
7.23
7.22
6.61
6.59
6.52
3.45
3.43
3.41
3.39
1.23
1.21
1.20
0.99
1.02
1.98
0.93
1.00
0.97
4.05
5.92
f1 (ppm)

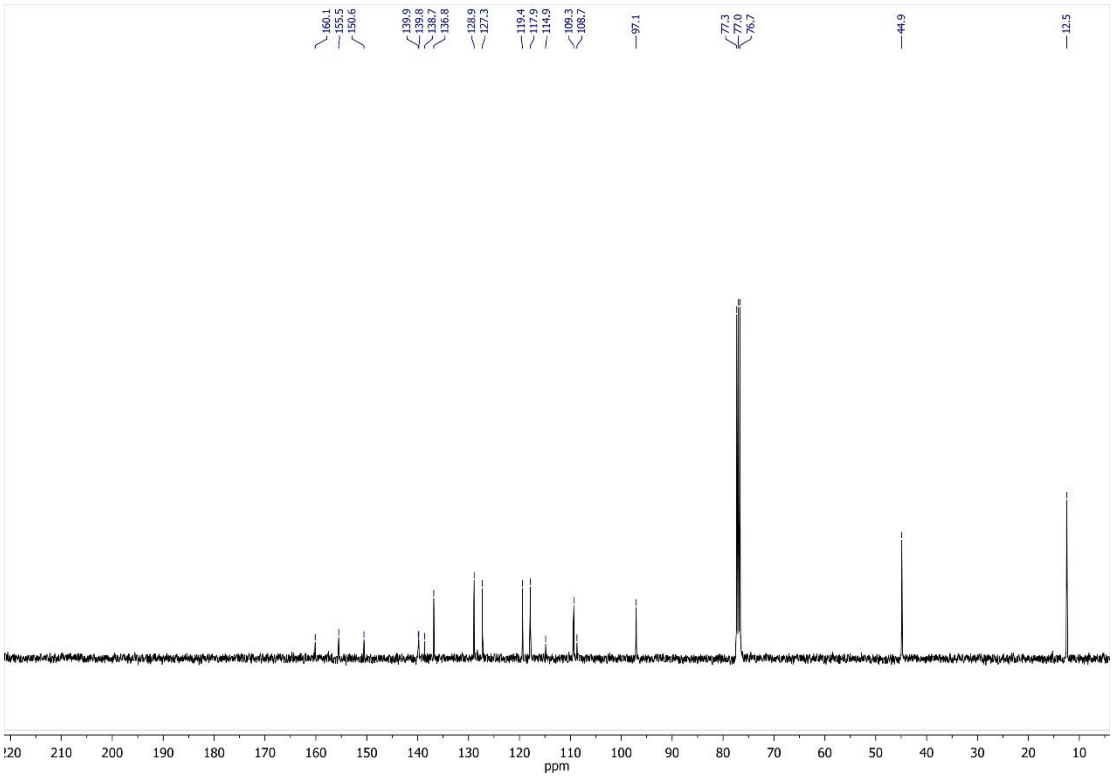
160.1
155.5
150.6
139.9
139.8
138.7
136.8
128.9
127.3
119.4
117.9
114.9
109.3
108.7
97.1
77.3
77.0
76.7
44.9
12.5
ppm

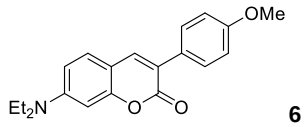
OMe
Et2N
O
O

**6**

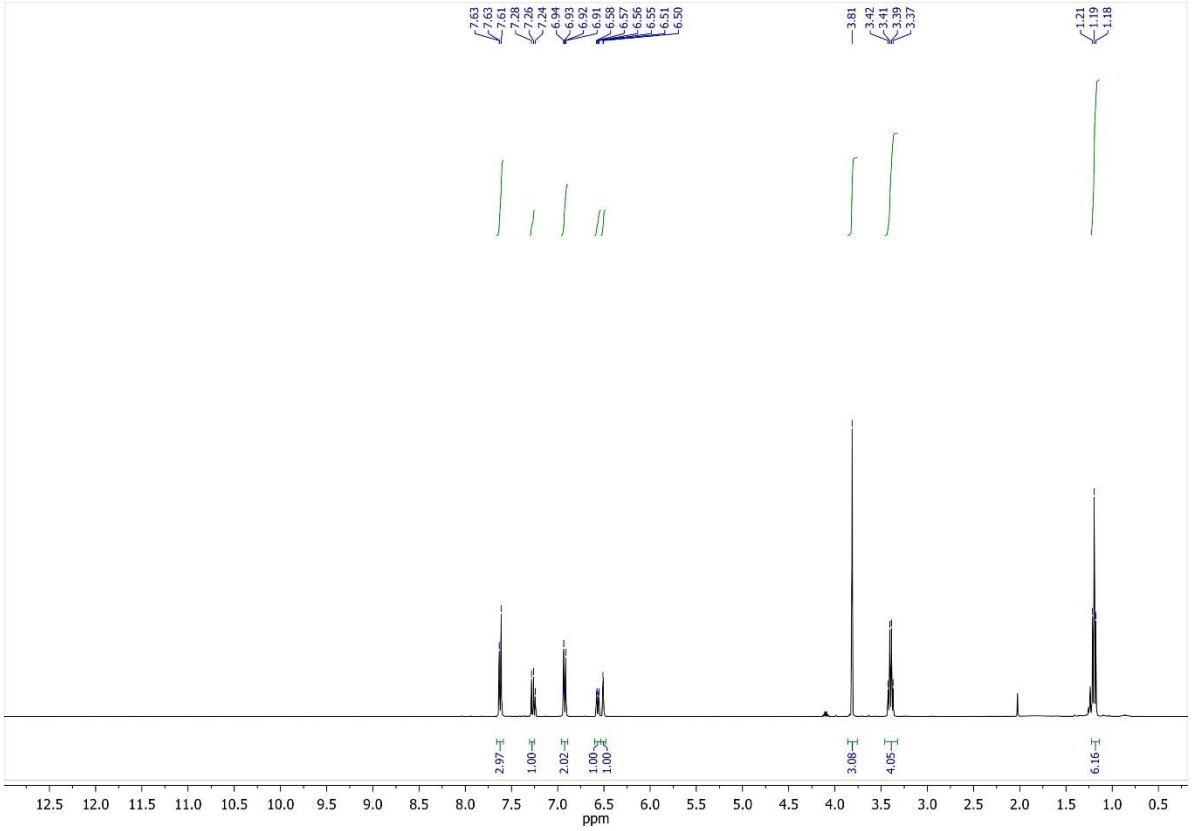
7.63
7.63
7.61
7.28
7.26
7.24
6.94
6.93
6.92
6.91
6.58
6.57
6.56
6.55
6.51
6.50
3.81
3.42
3.41
3.39
3.37
1.21
1.19
1.18
2.97
1.00
2.02
1.00
1.00
3.08
4.05
6.16
ppm

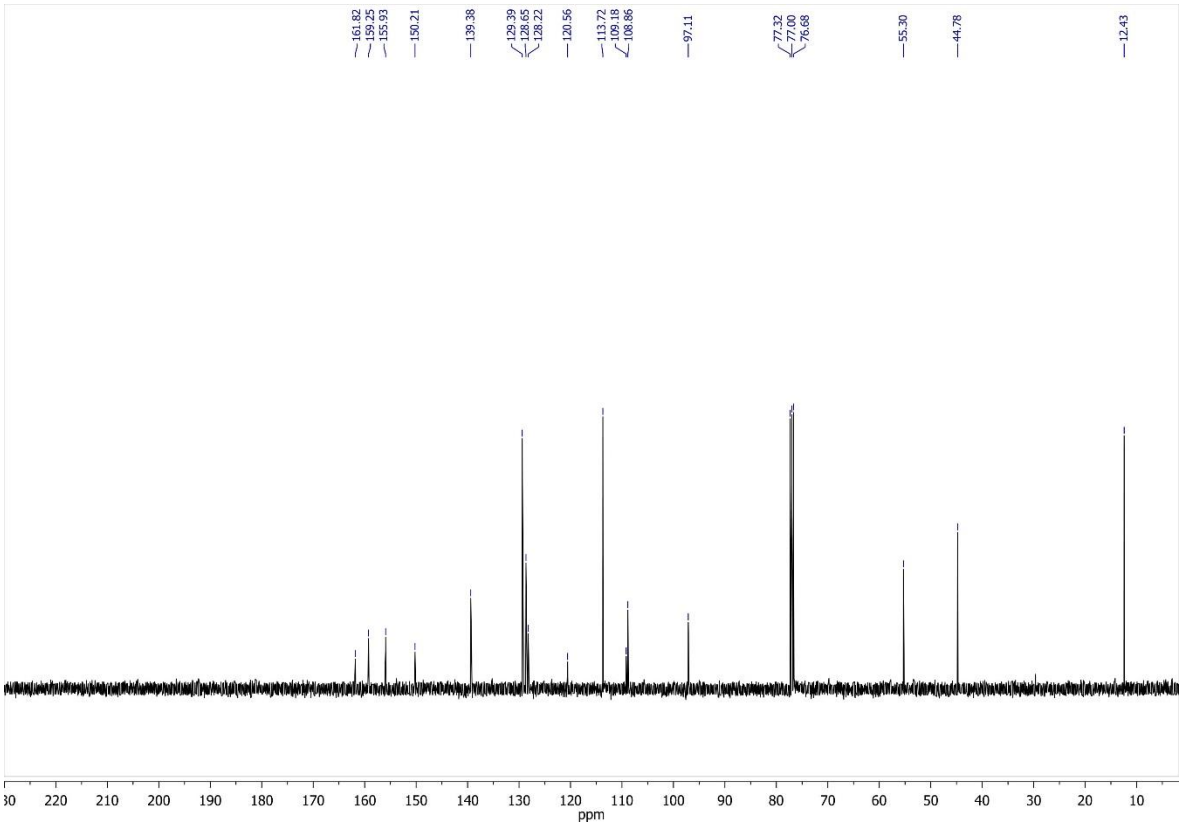
161.82
159.25
155.93
150.21
139.38
129.39
128.65
128.22
120.56
113.72
109.18
108.86
97.11
77.32
77.00
76.68
55.30
44.78
12.43
ppm

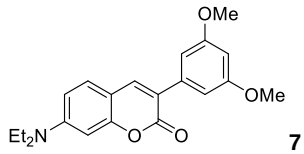
OMe
OMe
Et2N
O
O

**7**

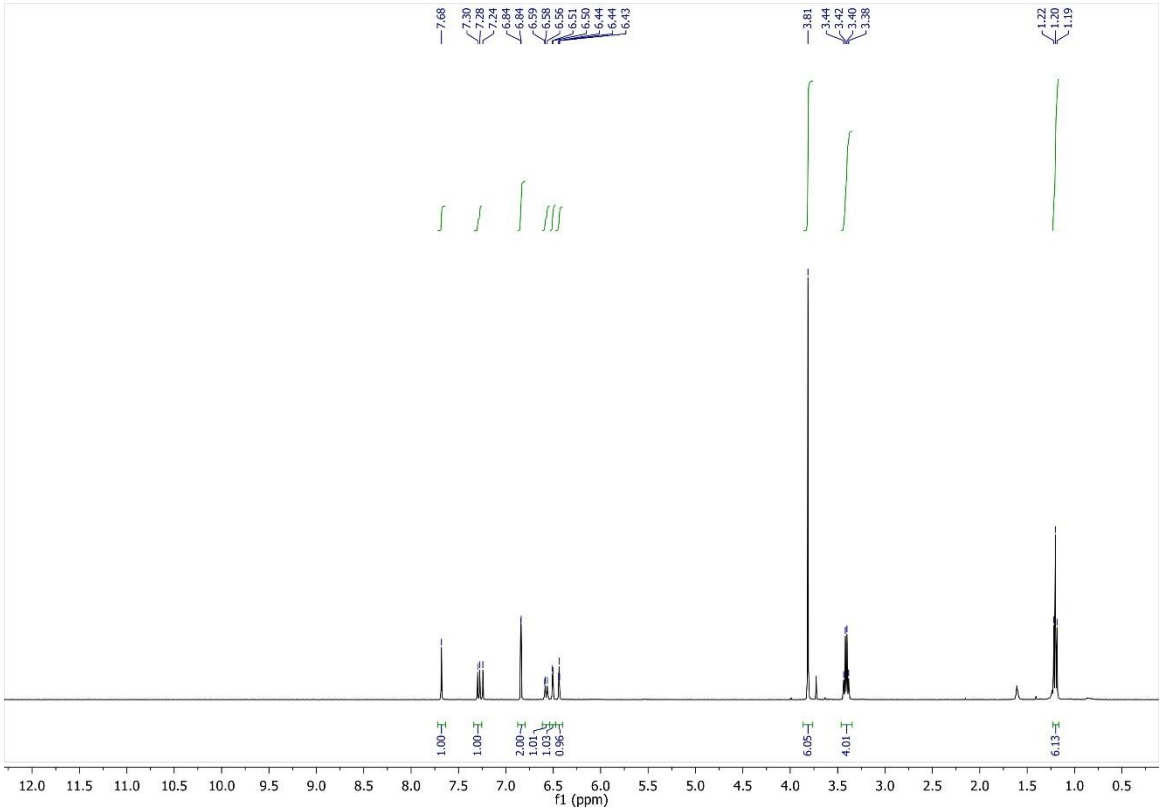
7.68
7.30
7.28
7.24
6.84
6.84
6.59
6.58
6.56
6.51
6.50
6.44
6.44
6.43
3.81
3.44
3.42
3.40
3.38
1.22
1.20
1.19
1.00
1.00
2.00
1.01
1.03
0.96
6.05
4.01
6.13
f1 (ppm)

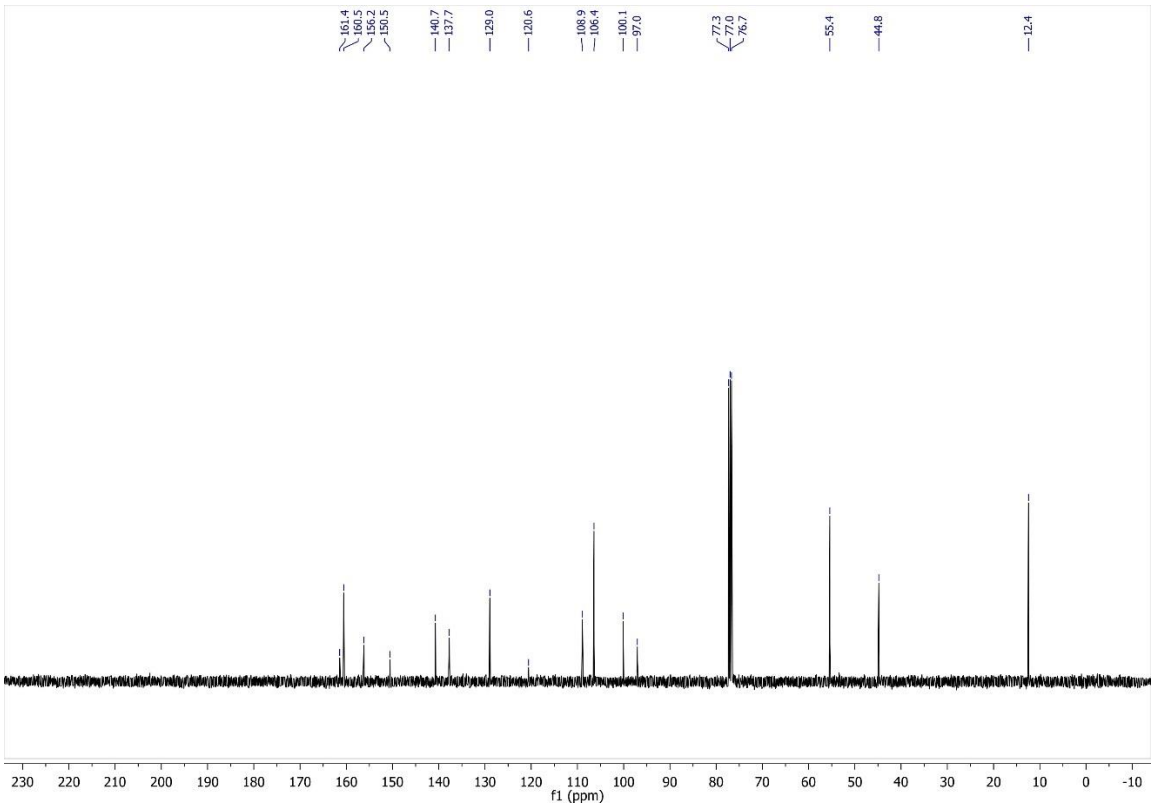
161.4
160.5
156.2
150.5
140.7
137.7
129.0
120.6
108.9
106.4
100.1
97.0
77.3
77.0
76.7
55.4
44.8
12.4
f1 (ppm)

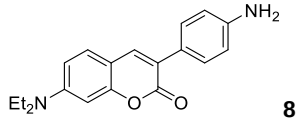
NH2
Et2N
O
O

**8**

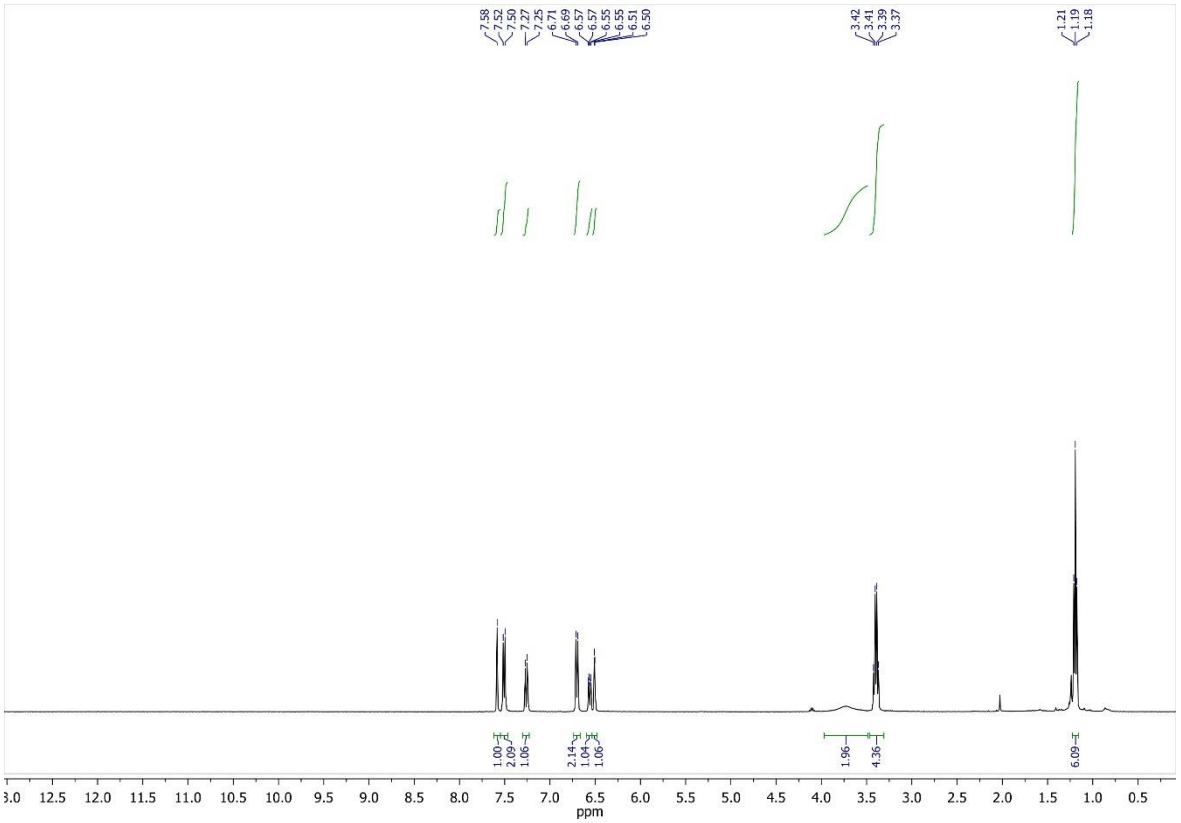
7.58
7.52
7.50
7.27
7.25
6.71
6.69
6.57
6.55
6.55
6.51
6.50
3.42
3.41
3.39
3.37
1.21
1.19
1.18
1.00
2.09
1.06
2.14
1.04
1.06
1.96
4.36
6.09
ppm

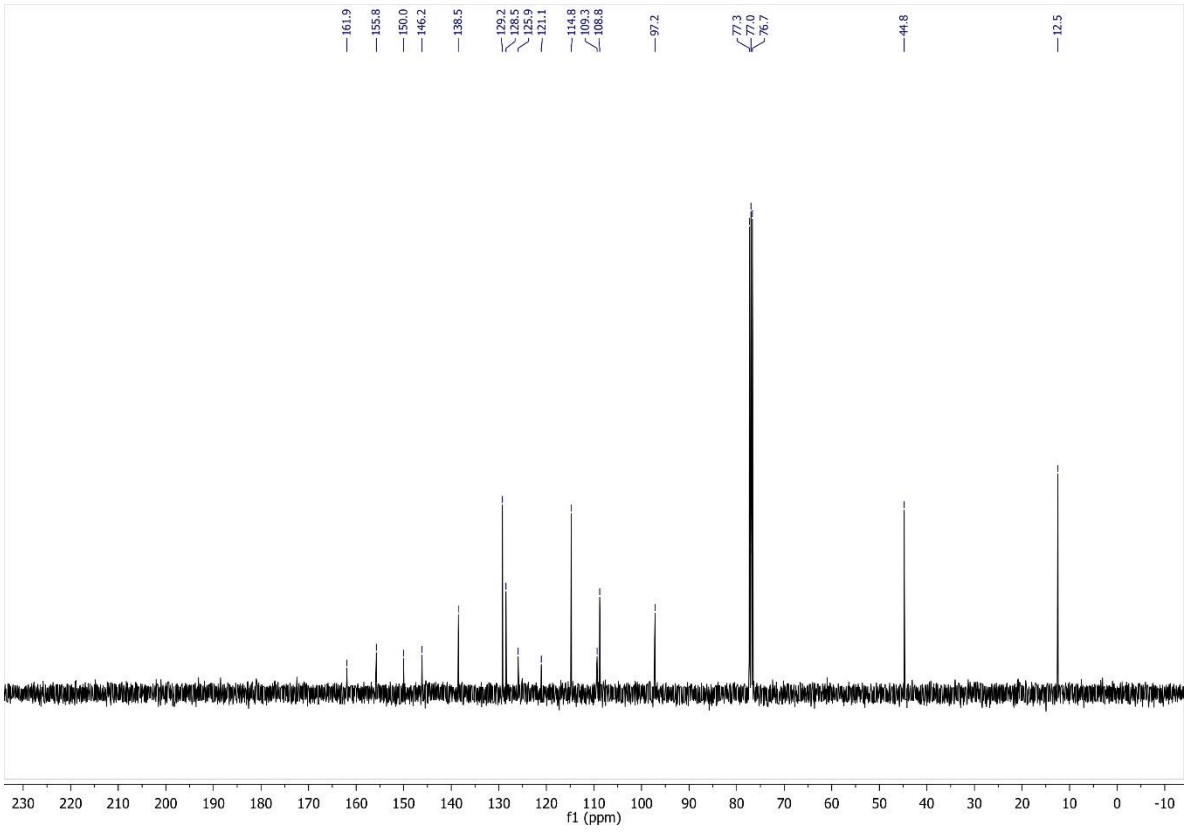
161.9
155.8
150.0
146.2
138.5
129.2
128.5
125.9
121.1
114.8
109.3
108.8
97.2
77.3
77.0
76.7
44.8
12.5
f1 (ppm)

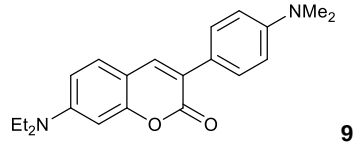
NMe2
Et2N
O
O

**9**

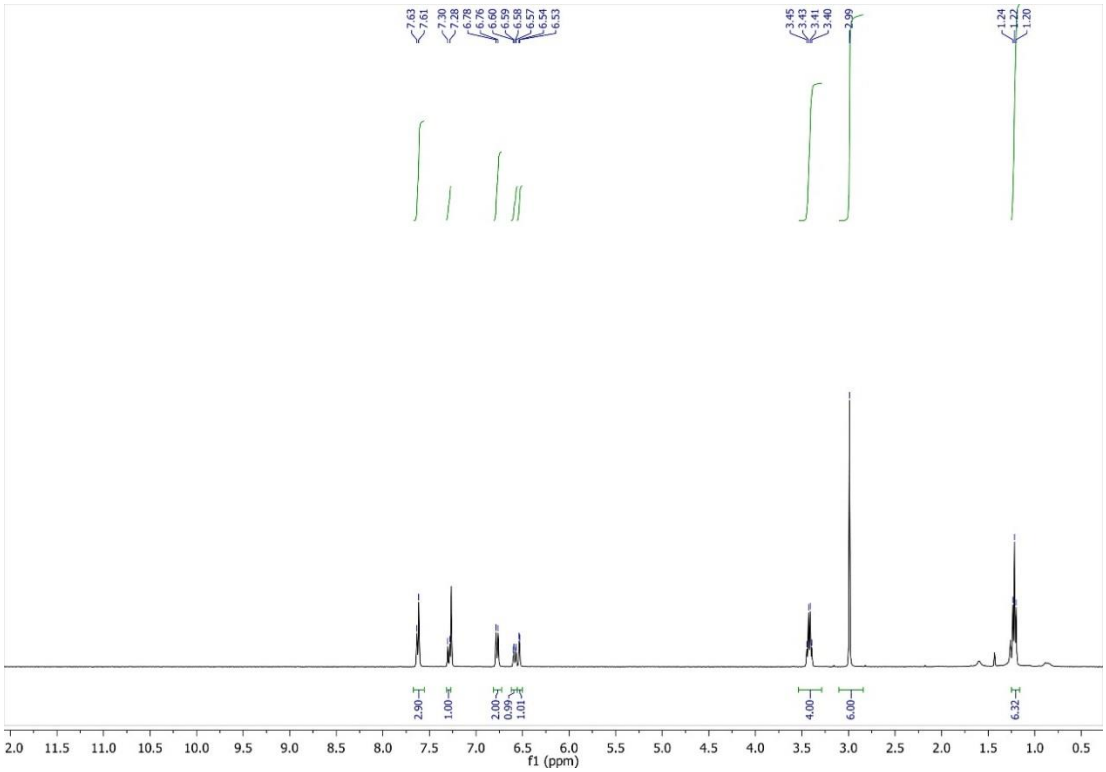
7.63
7.61
7.30
7.28
6.78
6.76
6.60
6.59
6.58
6.57
6.54
6.53
3.45
3.43
3.41
3.40
2.99
1.24
1.22
1.20
2.90
1.00
2.00
0.99
1.01
4.00
6.00
6.32
f1 (ppm)

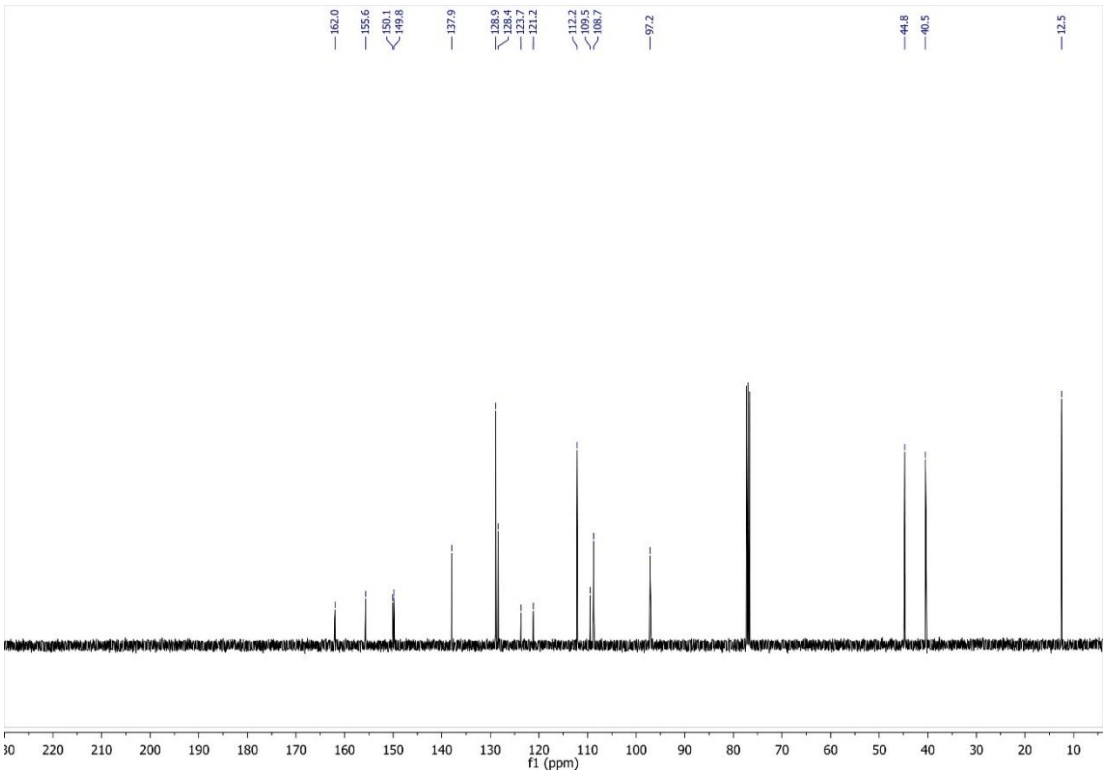
162.0
155.6
150.1
149.8
137.9
128.9
128.4
123.7
121.2
112.2
109.5
108.7
97.2
44.8
40.5
12.5
f1 (ppm)

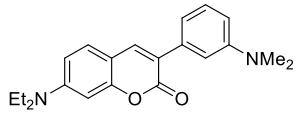
NMe2
Et2N
O
O

**10**

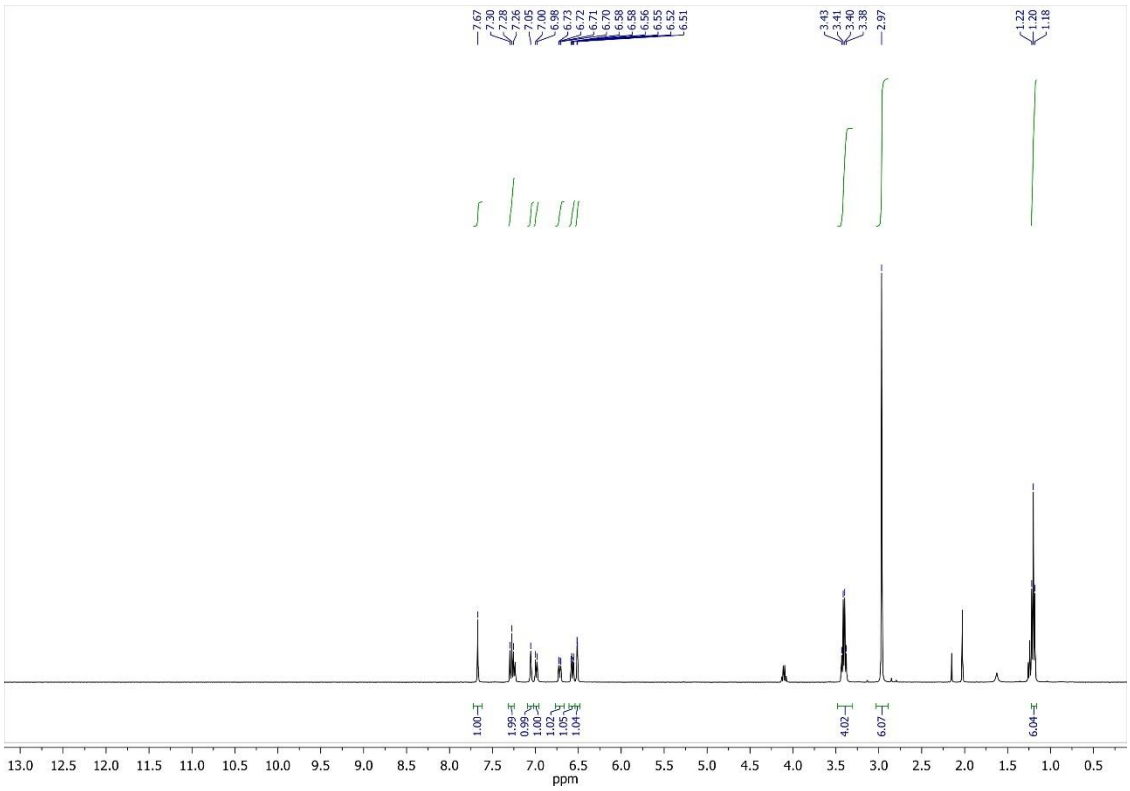
7.67
7.30
7.28
7.26
7.05
7.00
6.98
6.73
6.72
6.71
6.70
6.58
6.56
6.55
6.52
6.51
3.43
3.41
3.40
3.38
2.97
1.22
1.20
1.18
1.00
1.99
0.99
1.00
1.02
1.05
1.04
4.02
6.07
6.04
ppm

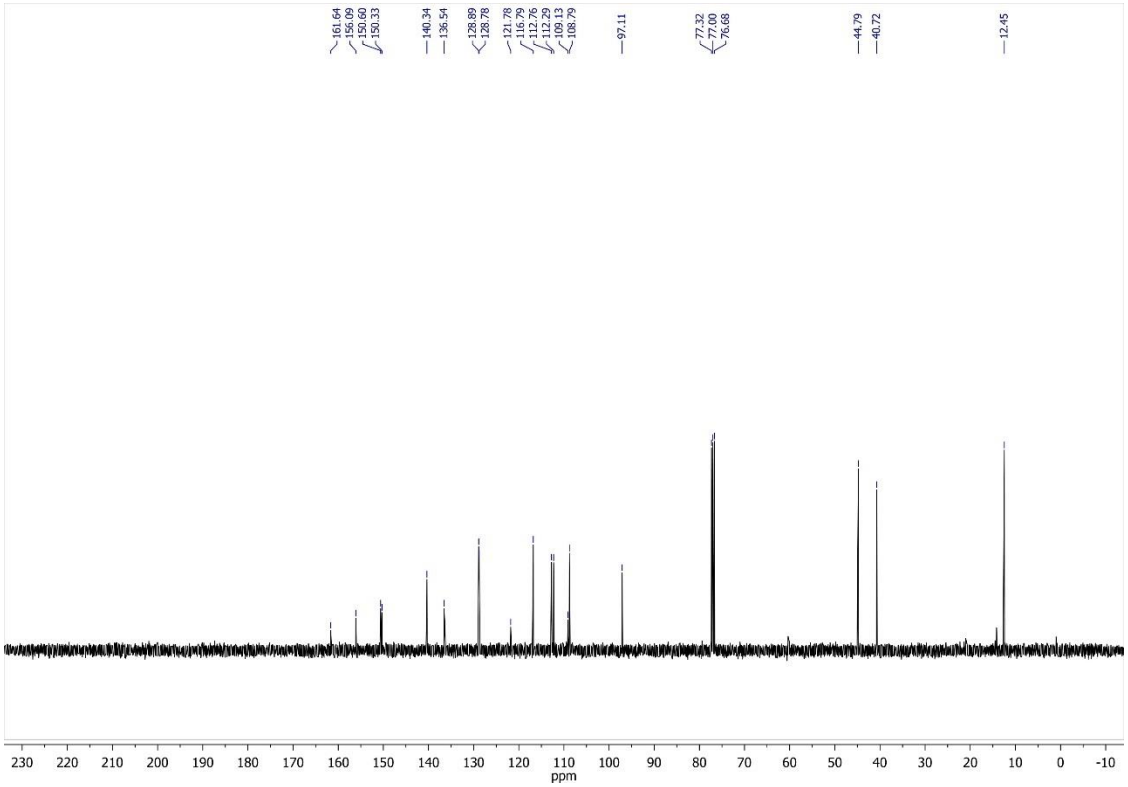
161.64
156.09
150.60
150.33
140.34
136.54
128.89
128.78
121.78
116.79
112.76
112.29
109.13
108.79
97.11
77.32
77.00
76.68
44.79
40.72
12.45
ppm

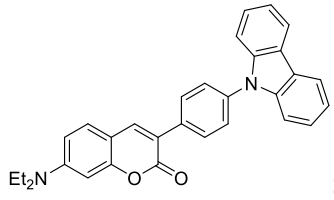
Et2N
O
O
N

**11**

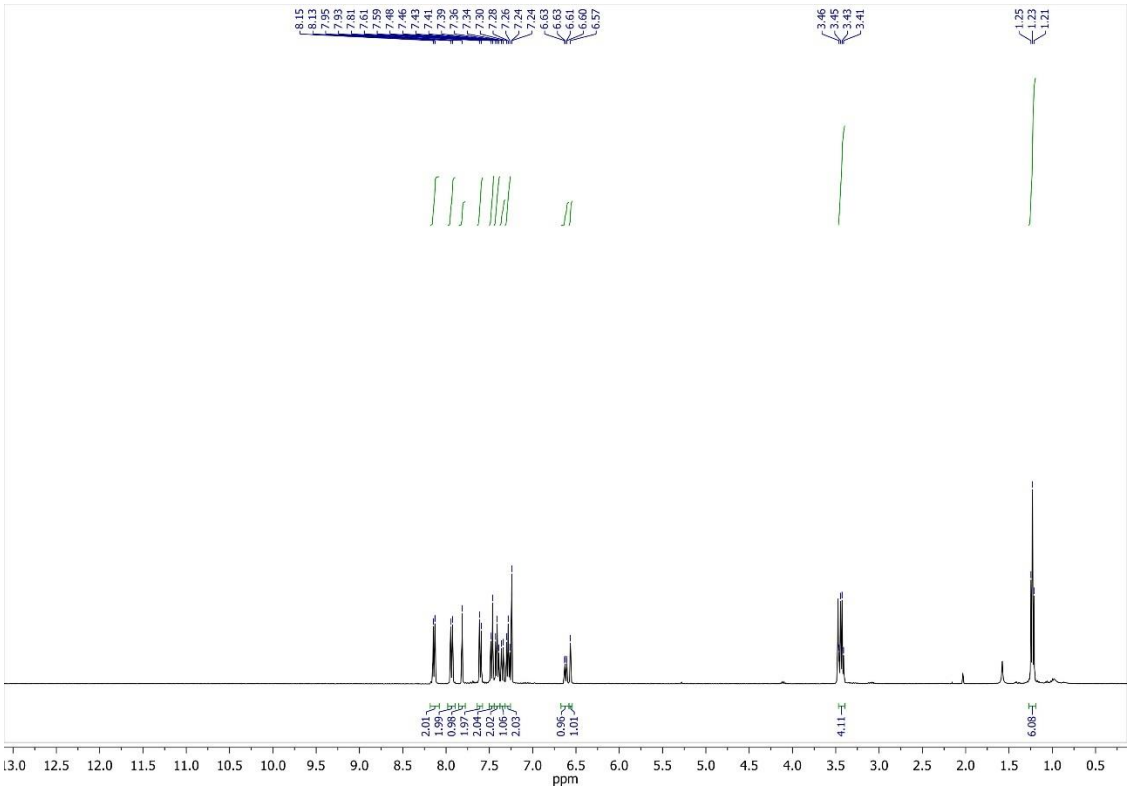
8.15
8.13
7.95
7.93
7.81
7.61
7.59
7.48
7.46
7.43
7.41
7.39
7.36
7.34
7.30
7.28
7.26
7.24
7.24
6.63
6.61
6.60
6.57
3.46
3.45
3.43
3.41
1.25
1.23
1.21
2.01
1.99
0.98
1.97
2.04
2.02
1.06
2.03
0.96
1.01
4.11
6.08
ppm

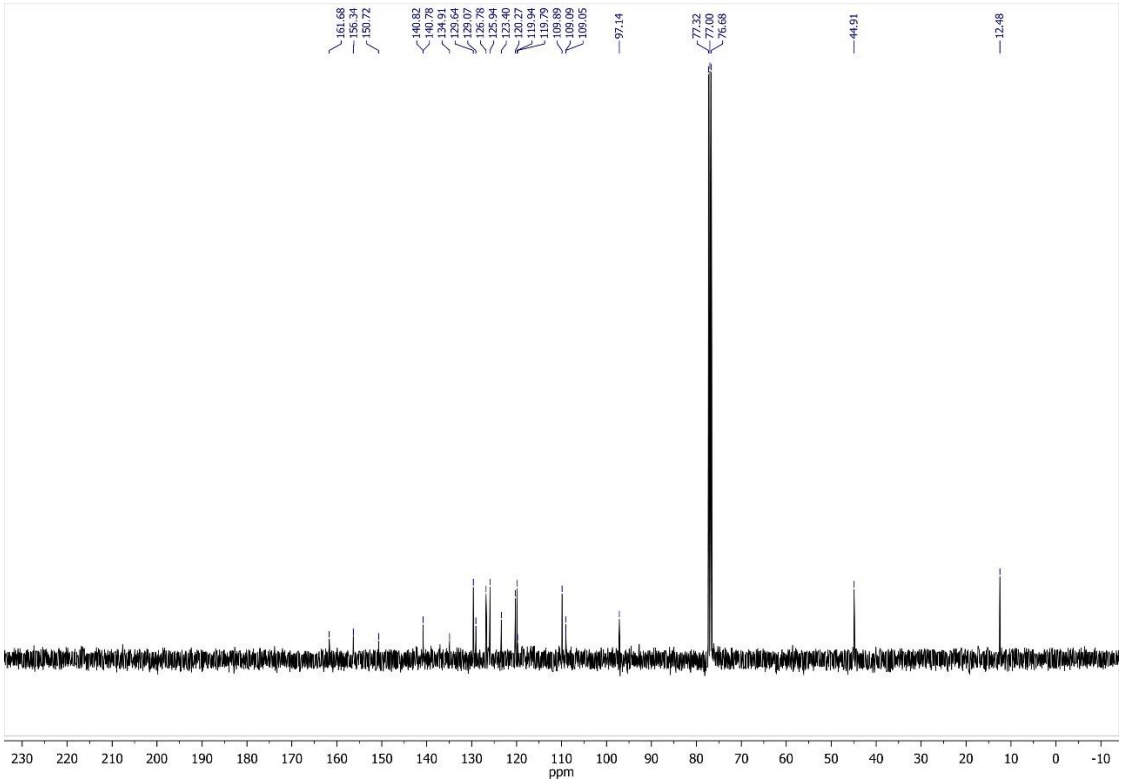
161.68
156.34
150.72
140.82
140.78
134.91
129.64
129.07
126.78
125.94
123.40
120.27
119.94
119.79
109.89
109.09
109.05
97.14
77.32
77.00
76.68
44.91
12.48
ppm

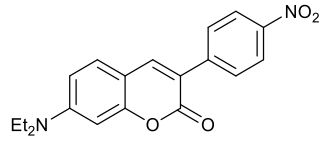
NO2
Et2N
O
O

**16**

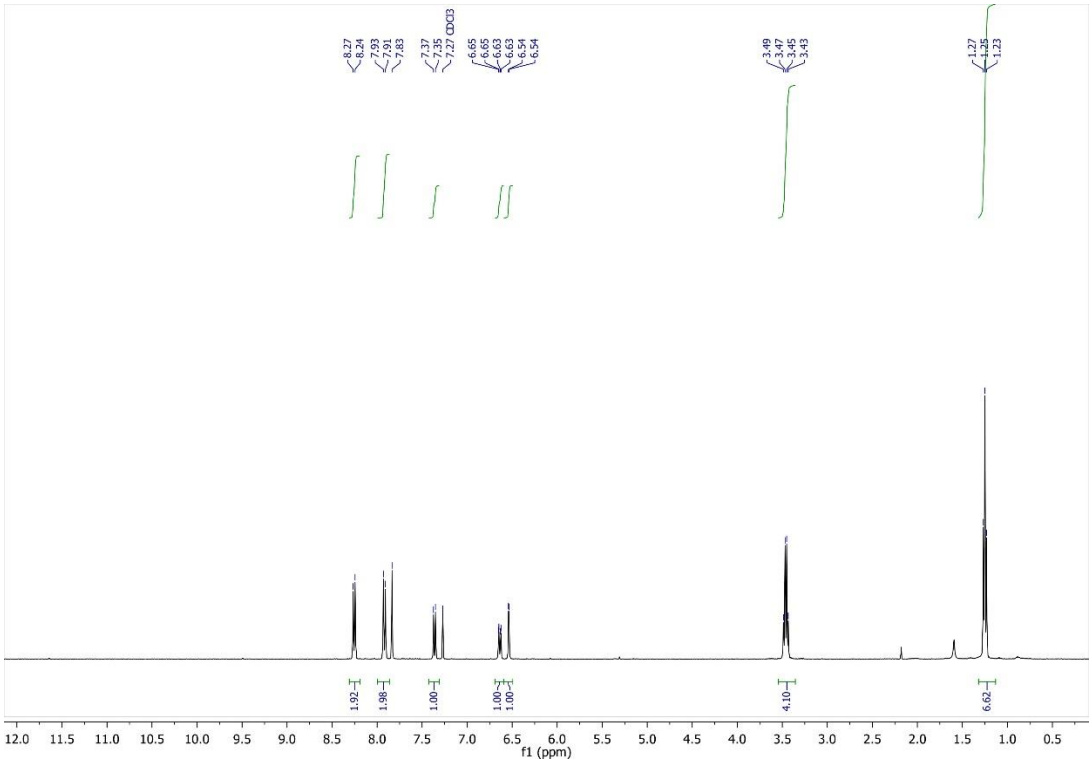
8.27
8.24
7.93
7.91
7.83
7.37
7.35
7.27 CDCl3
6.65
6.65
6.63
6.63
6.54
6.54
3.49
3.47
3.45
3.43
1.27
1.25
1.23
1.92
1.98
1.00
1.00
1.00
4.10
6.62
f1 (ppm)

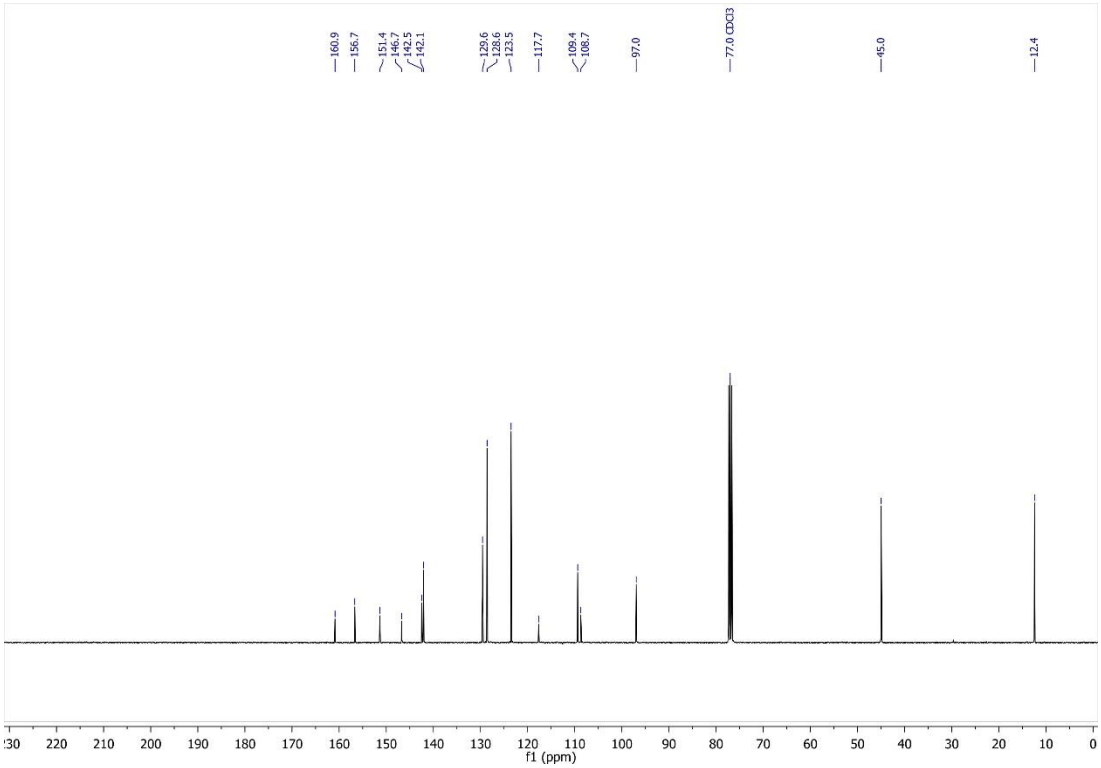
160.9
156.7
151.4
146.7
142.5
142.1
129.6
128.6
125.5
117.7
109.4
108.7
97.0
77.0 CDCl3
45.0
12.4
f1 (ppm)

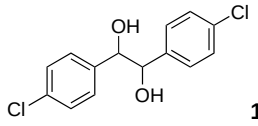
OH
Cl
Cl
OH

**18**

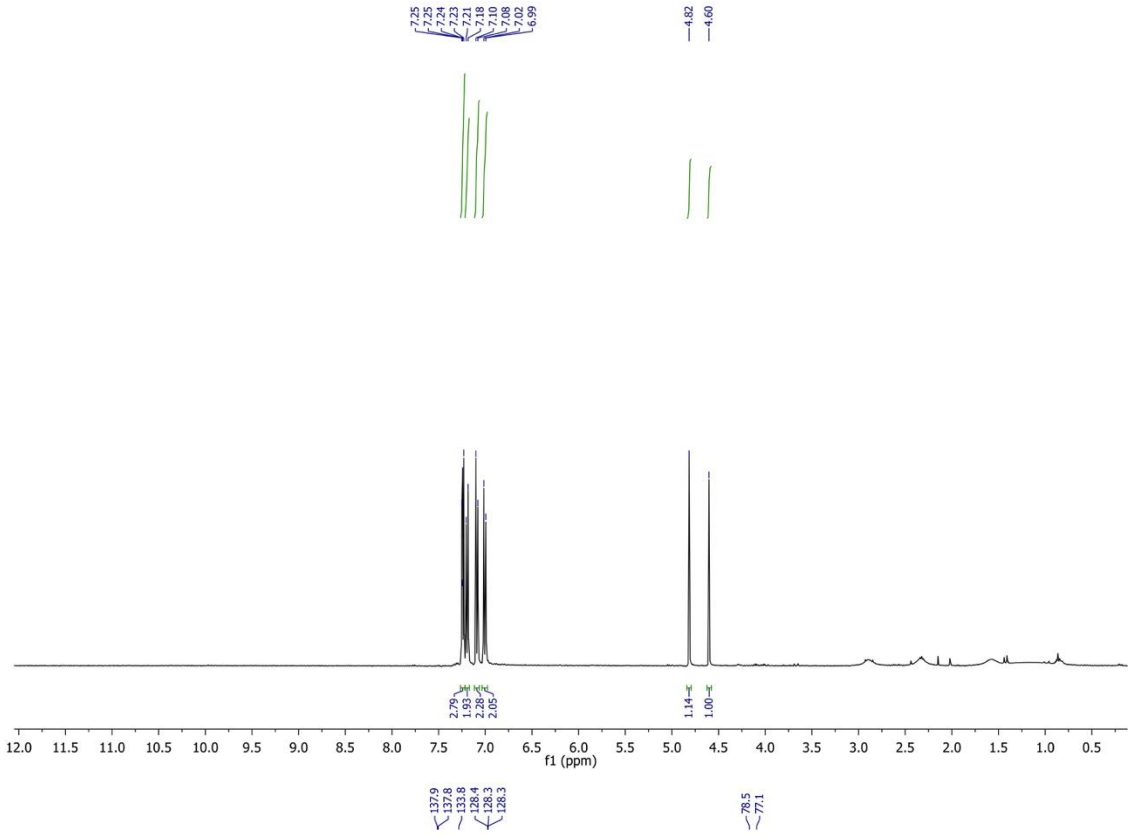
7.25
7.25
7.24
7.23
7.21
7.18
7.10
7.08
7.02
6.99
4.82
4.60
2.79
1.93
2.28
2.05
1.14
1.00
f1 (ppm)
137.9
137.8
133.8
128.4
128.3
128.3
78.5
77.1

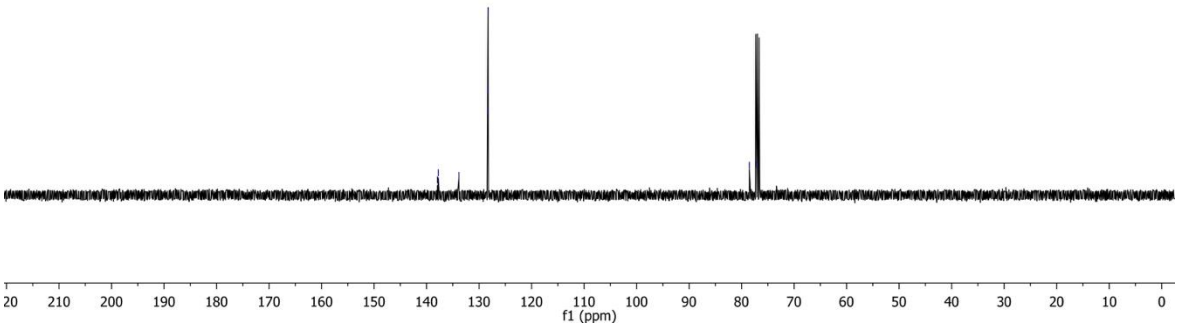
f1 (ppm)

## 3. Photophysical studies

**Figure S2**. On the left: absorption and emission spectra in DMF at 298 K; On the right: cyclic voltammetry of argon-purged solutions of coumarins in $CH_3CN$ in the presence of 0.1 M tetraethylammonium hexafluorophosphate ($TEAPF_6$). Scan rate=0.2 $Vs^{-1}$; working electrode: glassy carbon. The arrow shows the scanning direction of the cyclic voltammetry diagrams.

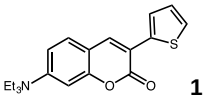


**1**

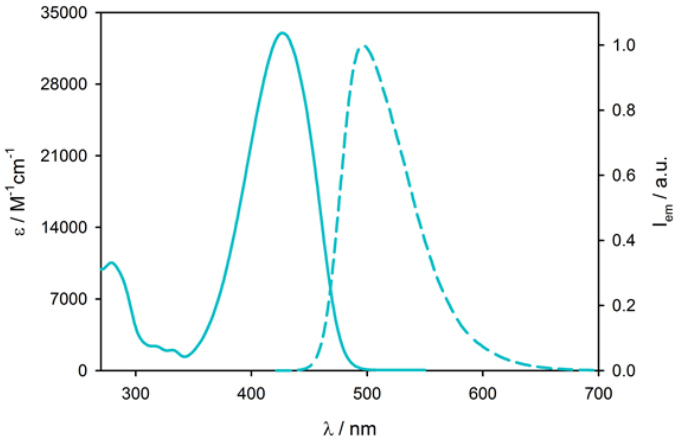


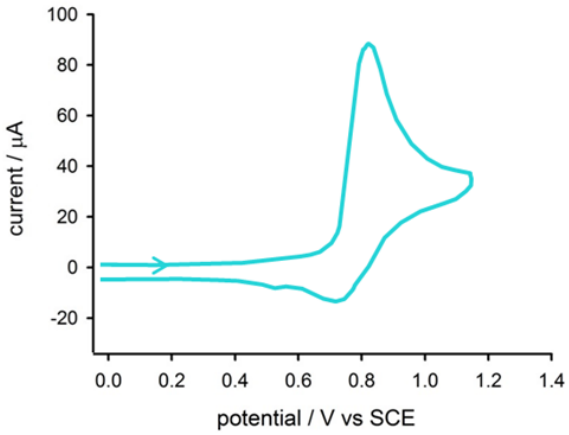


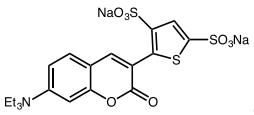


**2**

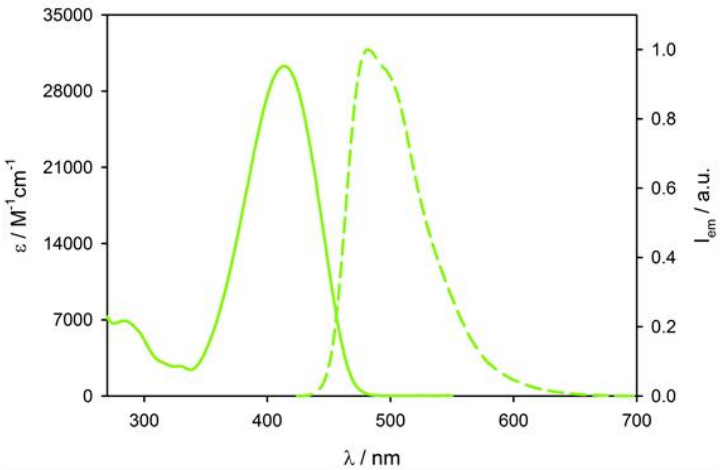


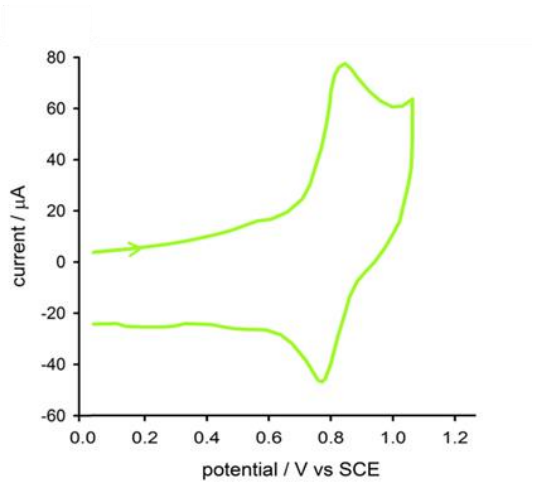

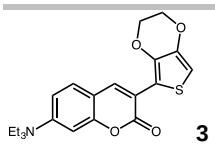
Et3N
O
O
O
S
O
O

**3**

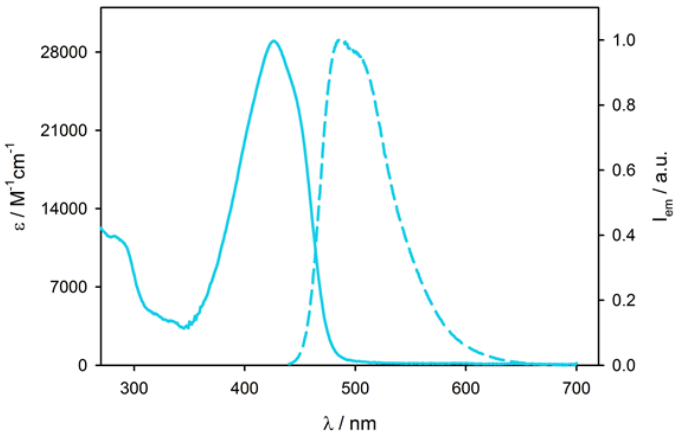
ε / M-1cm-1
Iem / a.u.
λ / nm
28000
21000
14000
7000
0
1.0
0.8
0.6
0.4
0.2
0.0
300
400
500
600
700

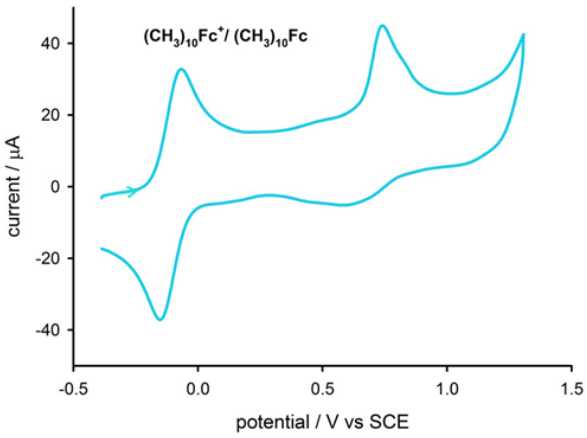
(CH3)10Fc+/ (CH3)10Fc
current / µA
potential / V vs SCE
40
20
0
-20
-40
-0.5
0.0
0.5
1.0
1.5

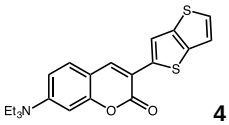
Et3N
O
O
S
S

**4**

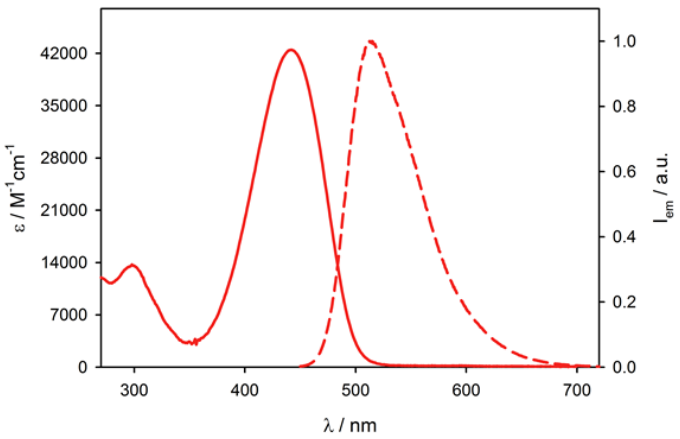
ε / M-1cm-1
Iem / a.u.
λ / nm
42000
35000
28000
21000
14000
7000
0
1.0
0.8
0.6
0.4
0.2
0.0
300
400
500
600
700

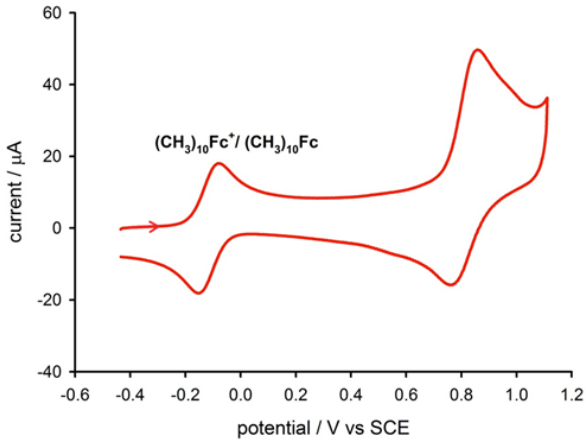
(CH3)10Fc+/ (CH3)10Fc
current / µA
potential / V vs SCE
60
40
20
0
-20
-40
-0.6
-0.4
-0.2
0.0
0.2
0.4
0.6
0.8
1.0
1.2

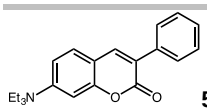
Et3N
O
O

**5**

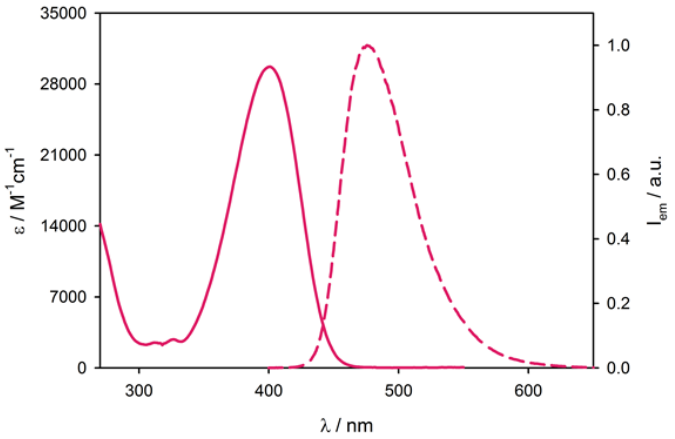
35000
28000
21000
14000
7000
0
ε / M-1cm-1
1.0
0.8
0.6
0.4
0.2
0.0
Iem / a.u.
300
400
500
600
λ / nm

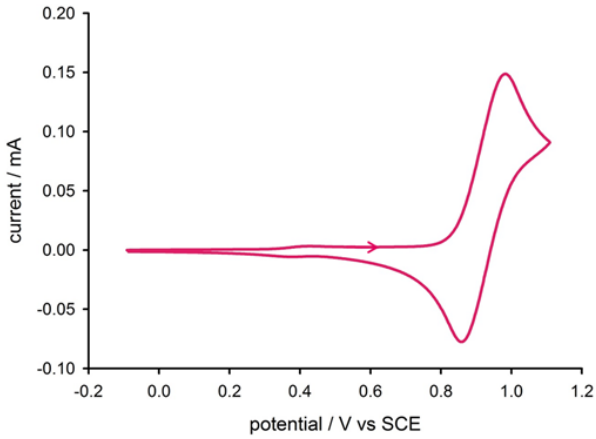
0.20
0.15
0.10
0.05
0.00
-0.05
-0.10
current / mA
-0.2
0.0
0.2
0.4
0.6
0.8
1.0
1.2
potential / V vs SCE

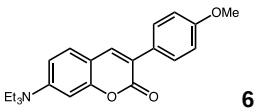
OMe
Et3N
O
O

**6**

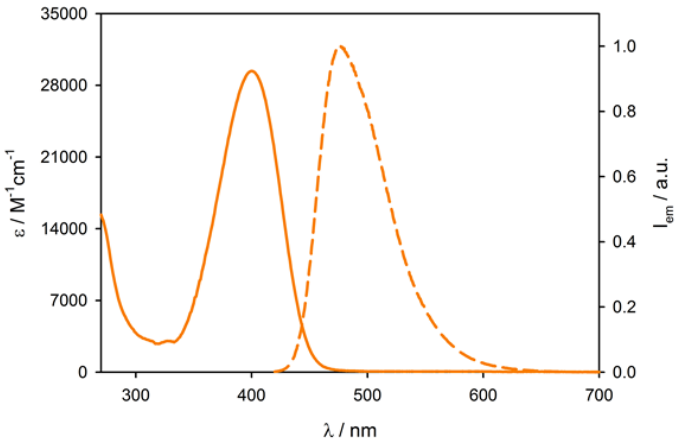
35000
28000
21000
14000
7000
0
ε / M-1cm-1
1.0
0.8
0.6
0.4
0.2
0.0
Iem / a.u.
300
400
500
600
700
λ / nm

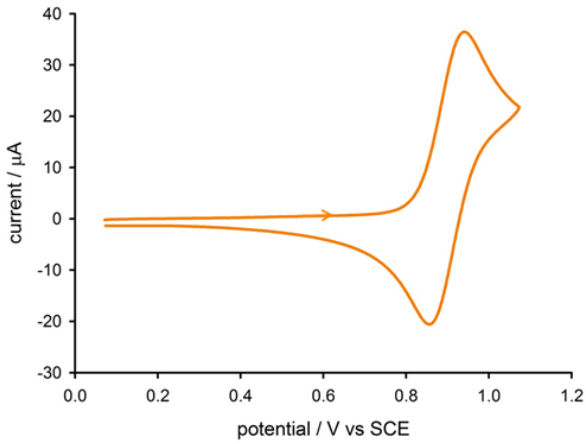
40
30
20
10
0
-10
-20
-30
current / µA
0.0
0.2
0.4
0.6
0.8
1.0
1.2
potential / V vs SCE

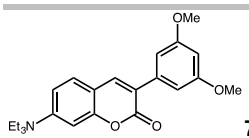
OMe
OMe
Et3N
O
O

**7**

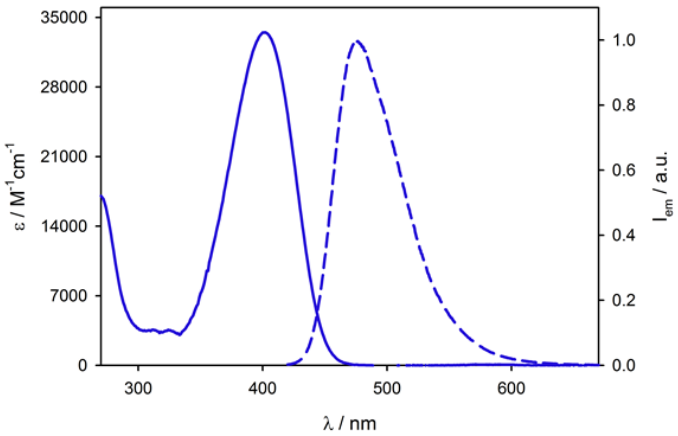
35000
28000
21000
14000
7000
0
ε / M-1cm-1
1.0
0.8
0.6
0.4
0.2
0.0
Iem / a.u.
300
400
500
600
λ / nm

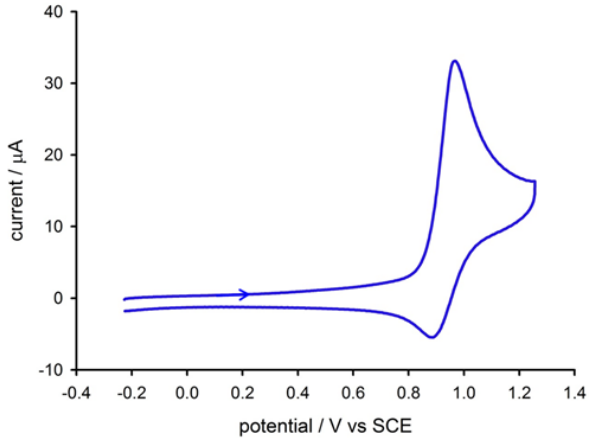
40
30
20
10
0
-10
current / µA
-0.4
-0.2
0.0
0.2
0.4
0.6
0.8
1.0
1.2
1.4
potential / V vs SCE

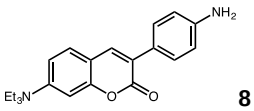
NH2
Et3N
O
O

**8**

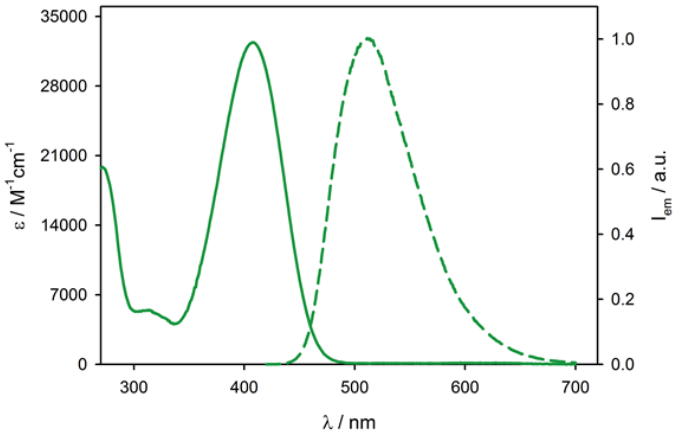
35000
28000
21000
14000
7000
0
ε / M-1cm-1
1.0
0.8
0.6
0.4
0.2
0.0
Iem / a.u.
300
400
500
600
700
λ / nm

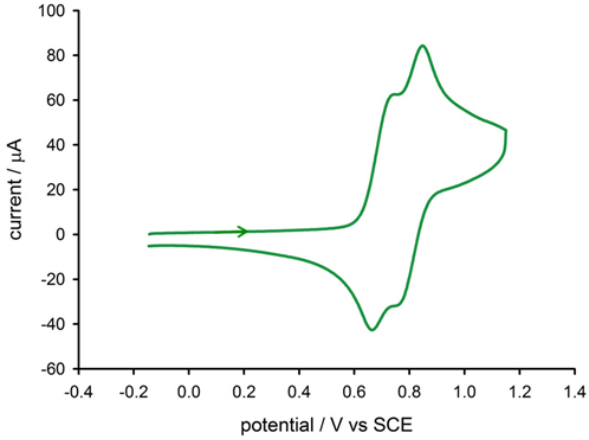
100
80
60
40
20
0
-20
-40
-60
current / µA
-0.4
-0.2
0.0
0.2
0.4
0.6
0.8
1.0
1.2
1.4
potential / V vs SCE

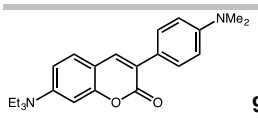
NMe2
Et3N
O
O

**9**

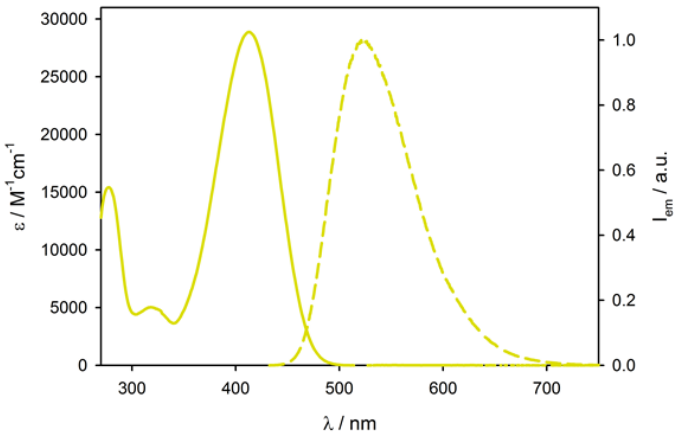
ε / M-1cm-1
Iem / a.u.
λ / nm

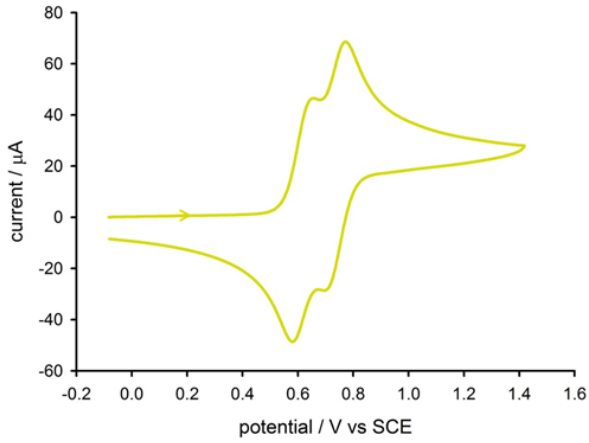
current / µA
potential / V vs SCE

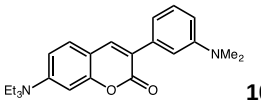
NMe2
Et3N
O
O

**10**

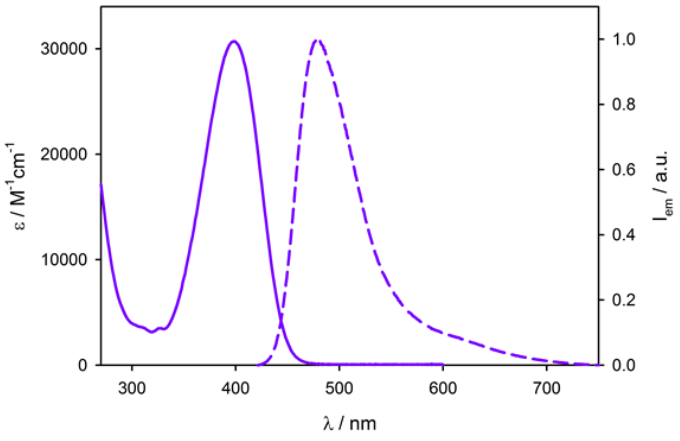
ε / M-1cm-1
Iem / a.u.
λ / nm

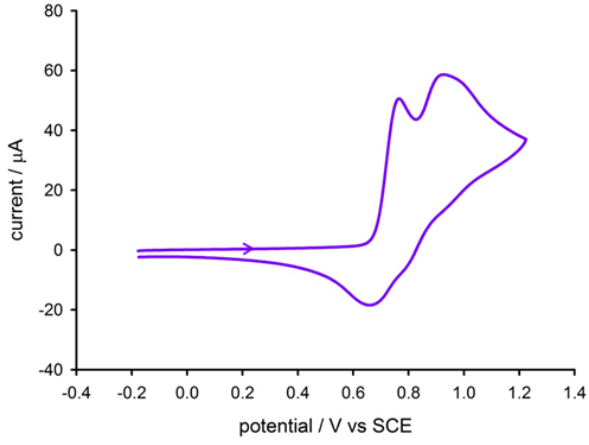
current / µA
potential / V vs SCE

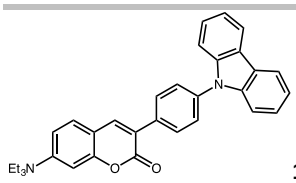


**11**

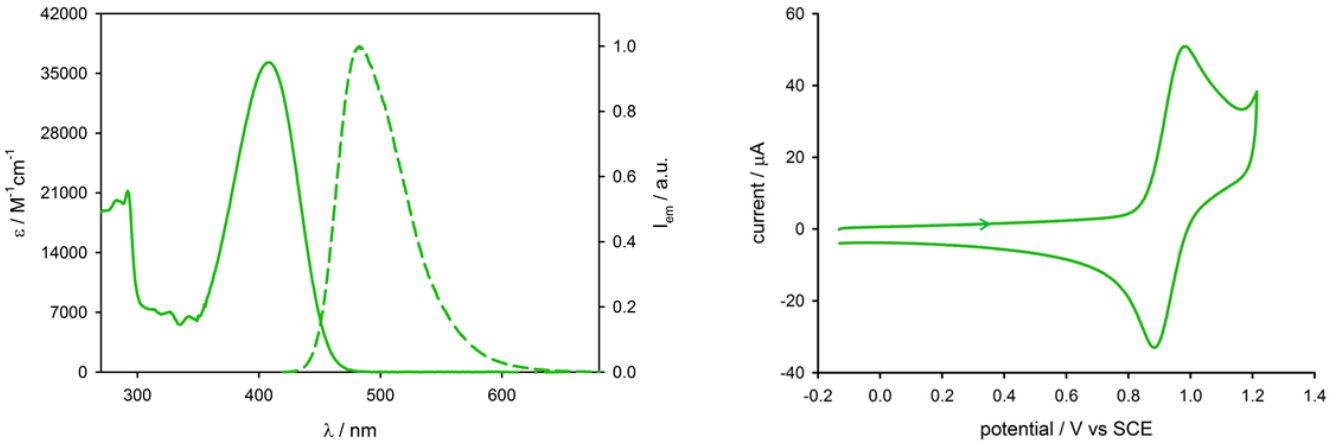


**Figure S3.** Cyclic Voltammetry of an argon-purged solution of **11** (1mM, black line) in DMF in the presence of 0. 1M tetraethylammonium tetrafluoroborate (TEATFB). Scan rate=0.2 $Vs^{-1}$; working electrode: glassy carbon; ferrocene (Fc) was used as internal standard. $E_{ox}$ (**11**$^{\bullet+}$/**11**) = +0.93 V vs SCE. The arrow shows the scanning direction of the cyclic voltammetry diagram.

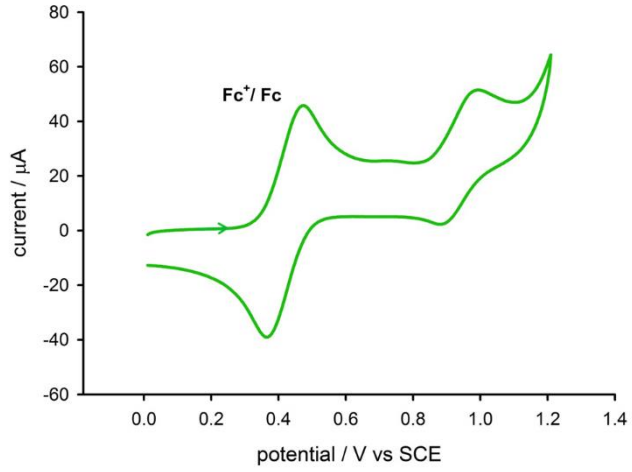

**Figure S4.** Cyclic Voltammetry of an argon-purged solution of TEA (triethylamine) (1mM) in $CH_3CN$ in the presence of 0.1M tetraethylammonium hexafluorophosphate (TE $APF_6$). Scan rate=0.2$Vs^{-1}$; working electrode: glassy carbon. The arrow shows the scanning direction of the cyclic voltammetry diagram.

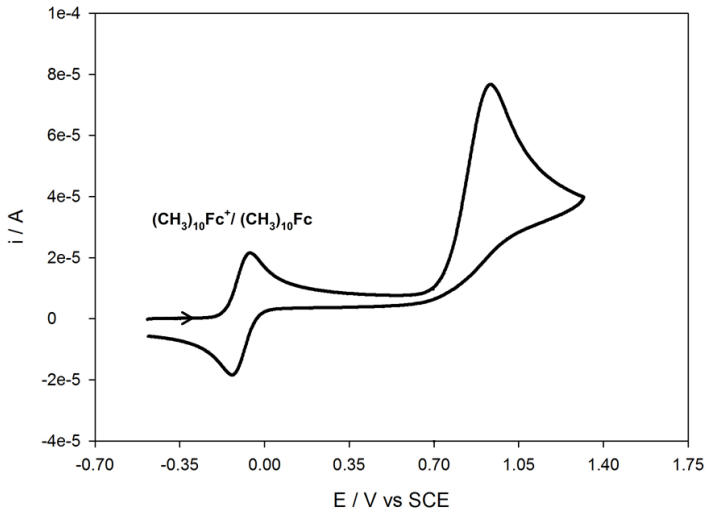


**Figure S5.** Absorption spectrum of the reaction mixture (diluted 1:100 before the collection of the spectrum) under standard conditions (chlorobenzaldehyde **17** 0.1M, TEA 0.3 M and coumarin **9** 0.005M in DMF) before (red solid line) and upon 24 hours irradiation with blue LEDs (black solid line).

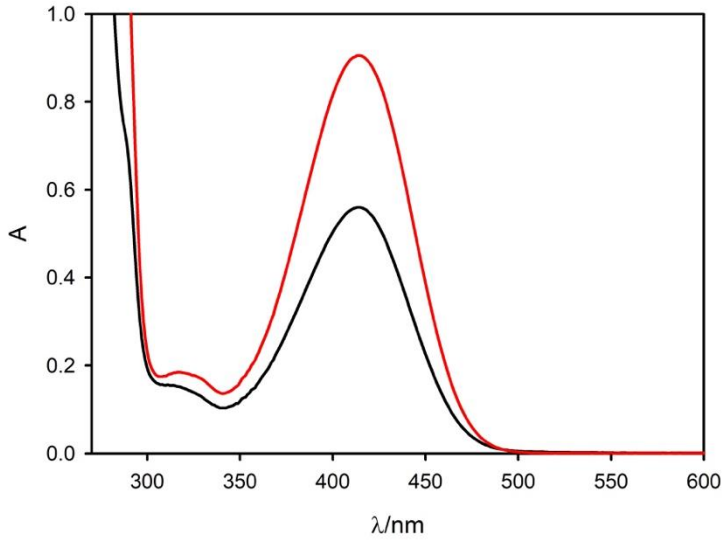

## 4. Computational Details

In the following we present the protocol for computing the oxidation potential $E^*_{ox}$. As outlined in the main text $E^*_{ox}$ depends on the ground state oxidation potential $E_{ox}$ (1) and the adiabatic excitation energy $E_{00}$ (2) according to the relation

$$E^*_{ox} = E_{ox} - E_{00}/nF$$

with $n$ is the number of electrons involved in the redox process (here equal to 1) and $F$ is the Faraday constant (equal to the unit charge e if the employed unit of energy is eV).

**(1) Ground state oxidation potential $E_{ox}$ in solution**

$E_{ox}$ was computed by two different protocols: a) a direct one which computes the Gibbs free energy change between the neutral form and the radical cation in solution-phase; and b) over a thermodynamic cycle by combining gas-phase energetics with solvation free energies of the neutral form and the radical cation[13]

**(a) Direct protocol**

The oxidation potential can be retrieved as the adiabatic Gibbs free energy of the solution-phase ionization $\Delta G_a(DMF)$ of the process $Cou(DMF) \rightarrow Cou^+(DMF)$

$$\begin{aligned}\Delta G_a(DMF) &= G@geom\big(Cou^+(DMF)\big) - G@geom\big(Cou(DMF)\big) \\ &= IP_a(DMF) + G_{therm}@geom\big(Cou^+(DMF)\big) - G_{therm}@geom\big(Cou(DMF)\big)\end{aligned}$$

The term $IP_a$ is the electronic contribution to the adiabatic ionization potential, the term $G_{therm} = ZPE + H - TS$ comprises the zero point energy (ZPE) and the thermal contribution of enthalpy ($H$) and entropy ($S$) at room temperature to the total energy of each species.
Since experimental redox potentials are not measured in isolation but are instead measured relative to the potential of a reference electrode we subtracted the redox potential of the reference electrode (e.g. saturated calomel electrode, SCE)

$$E_{ox} = \Delta G_a(DMF) - 4.35\ eV$$

where the last term is the standard redox potential of the SCE in DMF.[14]

**(b) Thermodynamic cycle**

The oxidation potential is defined as the Gibbs free energy change for a half-cell reaction. Specifically, the ground state redox potential can be retrieved in a three-step process

$$\begin{array}{ccc} Cou(DMF) & \rightarrow & Cou^+(DMF) \\ ①\ solvation \downarrow & & \uparrow ③\ solvation \\ Cou(g) & \xrightarrow{②\ ionization} & Cou^+(g) \end{array}$$

In ① the neutral system is brought from DMF to gas-phase, the thermodynamic quantity associated with this process is the solvation free energy $\Delta G_{solv}(Cou)$:

$$\Delta G_{sovl}(Cou) = \Delta G_{sovl}@geom\big(Cou(DMF)\big) + E\big(Cou(g)\big)@geom\big(Cou(DMF)\big)^1 - E\big(Cou(g)\big)@geom\big(Cou(g)\big)^2$$

where the second and third terms introduce a correction due to the conformational change associated with solvation.
In ② the neutral system is ionized, the thermodynamic quantity associated with this process is the adiabatic Gibbs free energy of the gas-phase ionization $\Delta G_a(g)$, which is the difference of Gibbs free energies of cation and neutral species

$$\begin{aligned}\Delta G_a(g) &= G@geom\big(Cou^+(g)\big) - G@geom\big(Cou(g)\big) \\ &= IP_a(g) + G_{therm}@geom\big(Cou^+(g)\big) - G_{therm}@geom\big(Cou(g)\big)\end{aligned}$$

In ③ the cation is brought from gas-phase to DMF, the thermodynamic quantity associated with this process is the solvation free energy $\Delta G_{solv}(Cou^+)$:

$$\Delta G_{solv}(Cou^+) = \Delta G_{sovl}@geom\big(Cou^+(DMF)\big) + E\big(Cou^+(g)\big)@geom\big(Cou^+(DMF)\big) - E\big(Cou^+(g)\big)@geom\big(Cou^+(g)\big)$$

[1] The notation implies that the gas-phase electronic energy $E\big(Cou(g)\big)$ is computed at the geometry relaxed in the presence of the solvent $geom\big(Cou(DMF)\big)$.
[2] The notation implies that the gas-phase electronic energy $E\big(Cou(g)\big)$ is computed at the geometry relaxed in gas-phase $geom\big(Cou(g)\big)$.

Finally, the ground state oxidation potential can be computed by adding all three contributions.

$$E_{ox} = -\Delta G_{solv}(Cou) + \Delta G_a(g) + \Delta G_{solv}(Cou^+) - 4.35\ eV$$

Note that the first term enters with a negative sign because the process described in ① is the opposite of solvation.
Table **S2** compares the values obtained for $E_{ox}$ with both protocols (**a**) and (**b**). Both protocols give comparable results, the direct protocol (**a**) delivers values which can be up to 0.05 eV higher than their counterparts obtained with the thermodynamic cycle protocol (**b**). One can also appreciate the agreement with respect to the experiment. Protocol (**a**) gives a slightly better agreement with the experiment (average error 0.07 eV) compared to protocol (**b**) (average error 0.10 eV). Table **S2** also provides the values for the solvation free energies $\Delta G_{solv}(Cou)$ and $\Delta G_{solv}(Cou^+)$, as well as the value of the adiabatic Gibbs free energy of the gas-phase ionization $\Delta G_a(g)$. Compound **2** shows values which deviate substantially from the overall trend because it is a di-anion. Anions are characterized with higher solvation free energies and lower ionization potentials.

**Table S2**

| | Electrochemistry ($E_{ox}$) | | | | | |
|---|---|---|---|---|---|---|
| | exp. | theo. | | | | |
| | | (**a**) | (**b**) | | | |
| | | | $-\Delta G_{solv}(Cou)$ | $\Delta G_a(g)$ | $\Delta G_{solv}(Cou^+)$ | total |
| **1** | +0.79 | +0.74 | +0.67 | +6.64 | -2.26 | +0.70 |
| **2** | +0.83 | +0.75 | +6.93 | +1.53 | -3.37 | +0.74 |
| **3** | +0.72 | +0.61 | +0.80 | +6.41 | -2.26 | +0.60 |
| **4** | +0.81 | +0.73 | +0.73 | +6.47 | -2.18 | +0.67 |
| **5** | +0.92 | +0.88 | +0.73 | +6.88 | -2.42 | +0.84 |
| **6** | +0.90 | +0.78 | +0.78 | +6.64 | -2.30 | +0.77 |
| **7** | +0.93 | +0.88 | +0.85 | +6.76 | -2.43 | +0.83 |
| **8** | +0.70 | +0.60 | +0.89 | +6.40 | -2.37 | +0.57 |
| **9** | +0.62 | +0.53 | +0.82 | +6.24 | -2.24 | +0.47 |
| **10** | +0.71 | +0.73 | +0.81 | +6.52 | -2.27 | +0.71 |
| **11** | +0.93 | +0.87 | +1.05 | +6.59 | -2.45 | +0.85 |

**(2) Adiabatic excitation energy $E_{00}$**

$E_{00}$ is defined as the energy difference between the excited and ground state equilibrium geometries

$$E_{00} = E_{S1}@geom\big(Cou^*(g)\big) - E_{S0}@geom\big(Cou(g)\big)$$

In principle, a more accurate way to calculate the adiabatic energy would require including the difference of zero point energy and thermal contributions $\Delta G_{therm} = \Delta ZPE + \Delta H - T\Delta S$ between ground and excited state minima. However, as excited state frequency calculations are very demanding, we adopt the displaced harmonic oscillator approximation, which assumes that the above contributions are identical for both states so that $\Delta G_{therm} = 0$.

All geometries were relaxed in gas-phase and in *N*,*N*-dimethylformamide (DMF, ε = 37.219) at the DFT level. The stationary nature of the optimized geometries was confirmed by frequency calculations. Excited state optimization was done with the time-dependent version of DFT on the first excited state which in all compounds is dominated by the HOMO → LUMO transition. The Minnesota exchange-correlation energy functional M06[15] in combination with the 6-311+G* basis set were utilized throughout. The SMD variation of integral-equation-formalism polarizable continuum model (IEFPCM) of Truhlar and workers[16] was used to treat solvent effects. The SMD model separates the observable solvation free energy into two main components. The first component is the bulk electrostatic contribution. The second component is called the cavity-dispersion-solvent-structure term and is the contribution arising from short-range interactions between the solute and solvent molecules in the first solvation shell. This makes SMD particularly suitable for computing solvation free energies $\Delta G_{solv}$. All calculations were performed with Gaussian 16.[17]

**Figure S6**. HOMO and LUMO orbitals involved in the electronic transition in the first excited state ($S_1$).

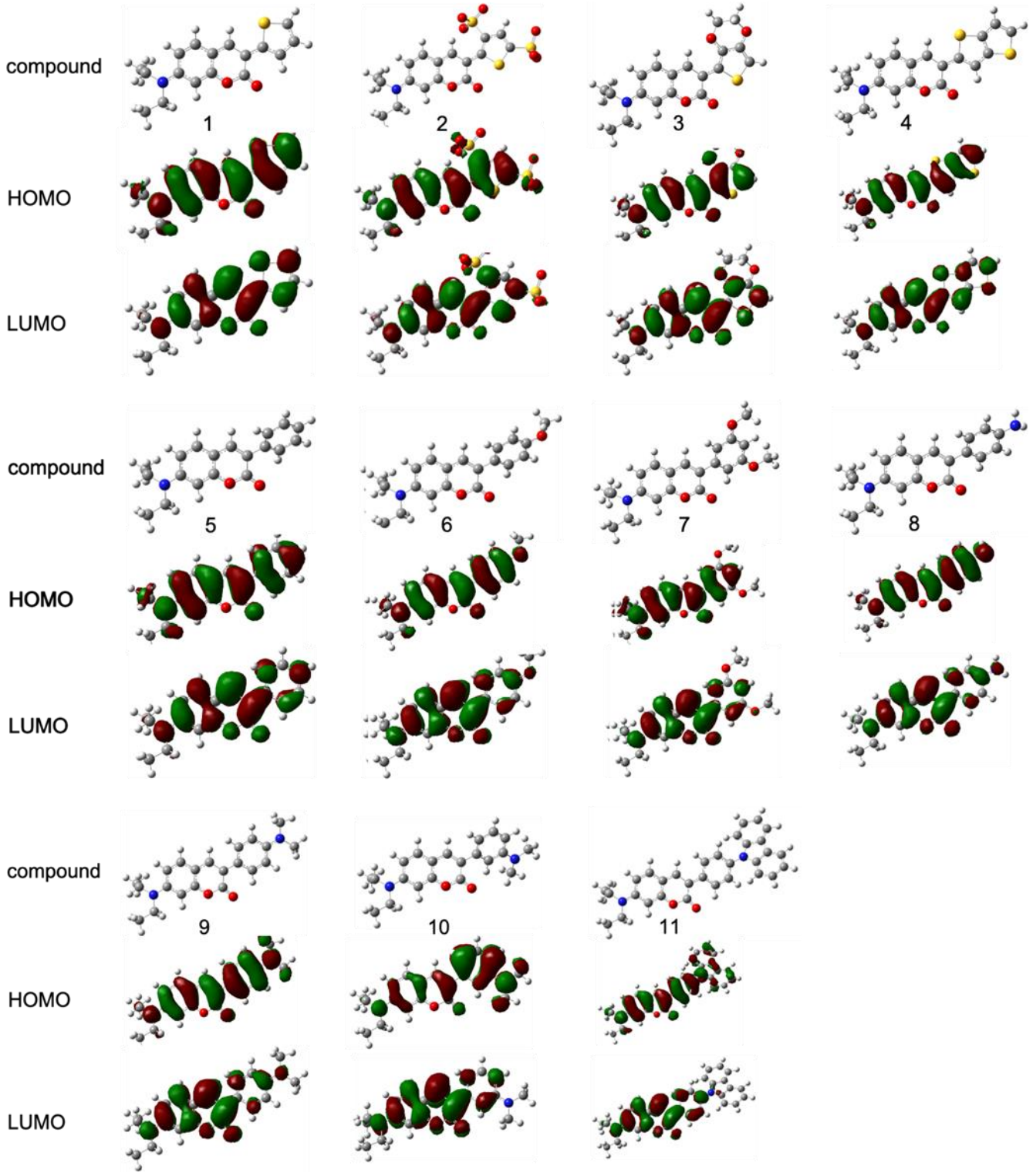

**Figure S7**. Electrostatic potential (ESP)-mapped electronic density for the radical cation (top) ground state (center) and first excited state (bottom) of each compound. Red and blue color indicate positive and negative values of the ESP, respectively. For all neutral species the ESP maps are plotted with limits [-0.05 : +0.05] a.u.. For all cations the ESP maps are plotted with limits [+0.05 : +0.15] a.u. For compound **2**, the ESP of the -2 charged species are plotted with limits [-0.25 : -0.03] a.u.. whereas the ESP of the -1 charged species is plotted with limits [-0.1 : +0.06] a.u.

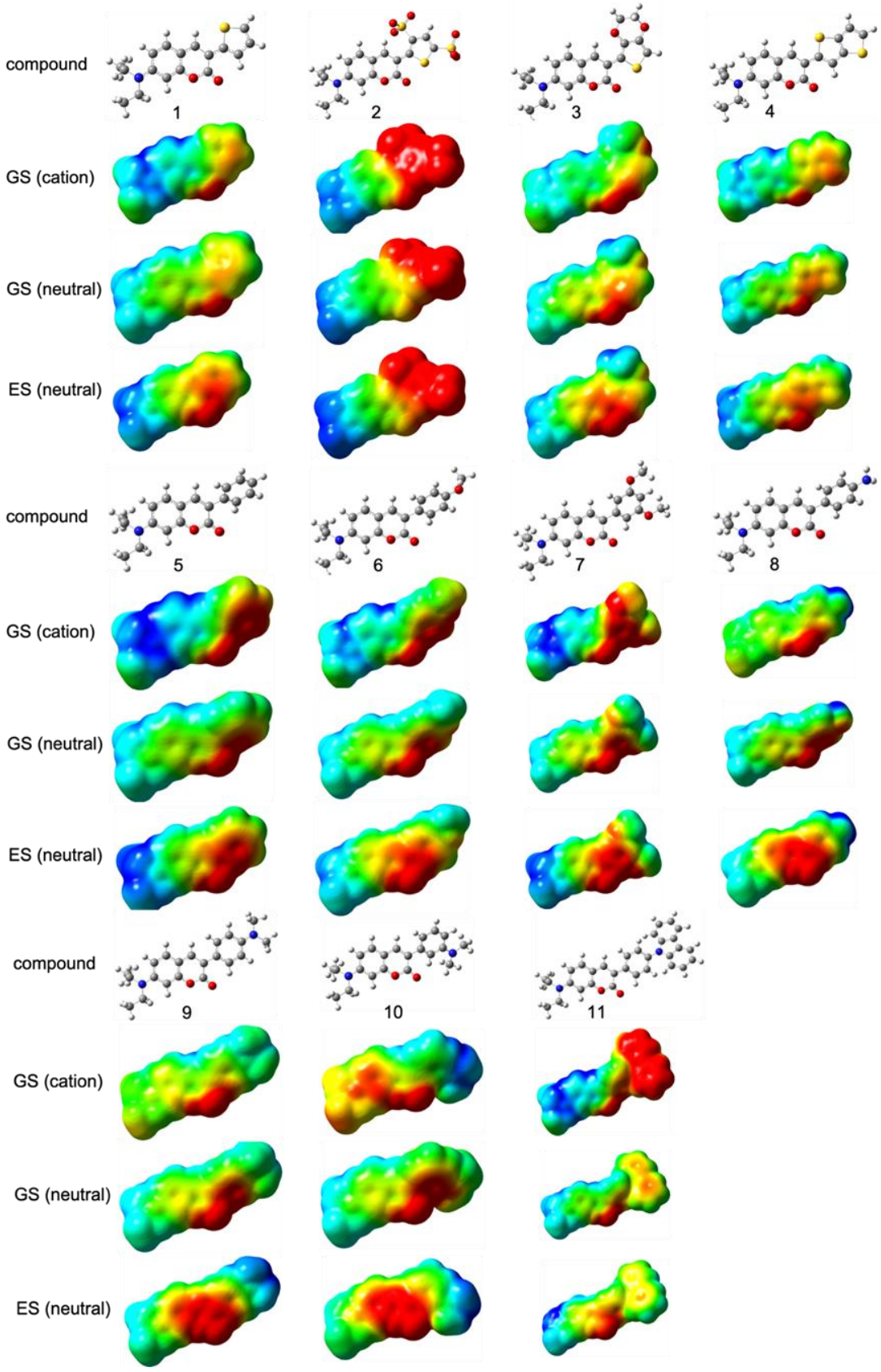

## 5. Discussion

**Figure S8.** Proposed catalytic cycle for reaction using TEA as sacrificial reductant.

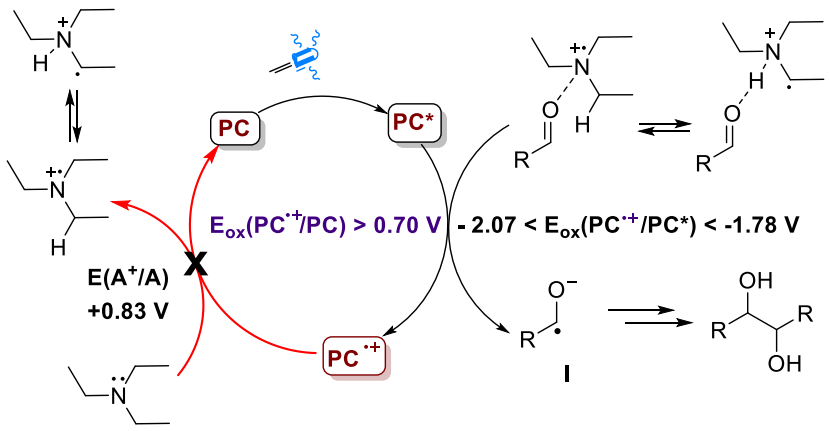


Our hypothesis of catalytic cycle (figure S7) is following the proposals discussed in publication by Rueping[18] and us.[1]
The photocatalyst in its excited state engages a SET with the carbonyl compound (as suggested by the Stern-Volmer analysis, fully described in our previous article[1]), generating the corresponding ketyl radical, it which undergoes dimerization providing the final product. Considering the reduction potential of carbonyl compounds (for 4-chlorobenzaldehyde, -1.96 V vs SCE in THF[19]) and the oxidation potential of the PC in its excited state ($-2.07<E_{ox}(PC^{\bullet+}/PC^*<-1.78$ V vs SCE), the process is endergonic or slightly exergonic. We suppose that the oxidized form of the sacrificial reductant, namely $TEA^{\bullet+}$, is responsible of the feasibility of the process, activating carbonyl compound by a two-center/three-electron interaction or through H-bonding.
In the first SET event of the catalytic cycle, oxidized form of the photocatalyst $PC^{\bullet+}$ was formed and the sacrificial reductant (TEA), is in charge of reducing it, and restore the coumarin in its ground state. The process is exergonic if the ground state oxidation potential of photocatalyst ($E_{ox}(PC^{\bullet+}/PC)$) is higher compare to the oxidation potential of $Et_3N$ (0.91 V vs SCE, see Figure S4). For all the coumarins tested, $E_{ox}(PC^{\bullet+}/PC)$ is higher than this value except for the compounds **3**, **8**, **9**, and **10** ($0.70<E_{ox}(PC^{\bullet+}/PC)$ V vs SCE). The impossibility of being reduced by the TEA, means that the coupling reaction does not occur when these coumarins are used as PC, as the photocatalyst is not restored after the first SET.

## 6. References


[1] A. Gualandi, G. Rodeghiero, E. Della Rocca, F. Bertoni, M. Marchini, R. Perciaccante, T. P. Jansen, P. Ceroni, P. G. Cozzi, *Chem. Commun.* **2018**, *54*, 10044-10047.
[2] F. Jafarpour, S. Zarei, M. Barzegar Amiri Olia, N. Jalalimanesh and S. Rahiminejadan, *J. Org. Chem.* **2013**, *78*, 2957-2964.
[3] T. Leermann, F. R. Leroux, F. Colobert, *Org. Lett.* **2011**, *13*, 4479-4481.
[4] S. M. Elbert, P. Wagner, T. Kanagasundaram, F. Rominger, M. Mastalerz, *Chem. --Eur. J.* **2017**, *23*, 935-945.
[5] L. Wang, E. Ji, N. Liu, B. Dai, *Synthesis* **2016**, *48*, 737-750.
[6] L. Guo, K. F. Li, M. S. Wong, K. W. Cheah, *Chem. Commun.* **2013**, *49*, 3597-3599.
[7] S. Fan, J. You, Y. Miao, H. Wang, Q. Bai, X. Liu, X. Li, S. Wang, *Dyes and Pigments* **2016**, *129*, 34-42.
[8] H. Sun, H. Guo, W. Wu, X. Liu, J. Zhao, *Dalton Transactions* **2011**, *40*, 7834-7841.
[9] T. M. Ha Vuong, D. Villemin, H.-H. Nguyen, T. T. Le, T. T. Dang, H. Nguyen, *Chemistry – An Asian Journal* **2017**, *12*, 2819-2826.
[10] A. Sasmal, J. K. Bera, H. Doucet, J.-F. Soulé, *Eur. J. Org. Chem.* **2018**, 6114-6120.
[11] B. Zhang, C. Ge, J. Yao, Y. Liu, H. Xie, J. Fang, *J. Am. Chem. Soc.* **2015**, *137*, 757-769.
[12] G. R. Robertson, *Org. Synth.* **1922**, *2*, 57.
[13] J. Ho, M. L. Coote, C. J. Cramer, D. G. Truhlar in Organic Electrochemistry, 5th ed., edited by O. Hammerich and B. Speiser, CRC Press, Boca Raton, FL, **2016**, 229-259.
[14] A. A. Isse, A. Gennaro, J. *Phys. Chem. B* **2010**, *114*, 7894-7899.
[15] Y. Zhao, D. G. Truhlar, *Theor. Chem. Acc.* **2008**, *120*, 215-241.
[16] A. V. Marenich, C. J. Cramer, D. G. Truhlar, *J. Phys. Chem. B* **2009**, *113*, 18, 6378-6396.
[17] M. J. Frisch, G. W. Trucks, H. B. Schlegel, G. E. Scuseria, M. A. Robb, J. R. Cheeseman, G. Scalmani, V. Barone, G. A. Petersson, H. Nakatsuji, X. Li, M. Caricato, A. V. Marenich, J. Bloino, B. G. Janesko, R. Gomperts, B. Mennucci, H. P. Hratchian, J. V. Ortiz, A. F. Izmaylov, J. L. Sonnenberg, D. Williams-Young, F. Ding, F. Lipparini, F. Egidi, J. Goings, B. Peng, A. Petrone, T. Henderson, D. Ranasinghe, V. G. Zakrzewski, J. Gao, N. Rega, G. Zheng, W. Liang, M. Hada, M. Ehara, K. Toyota, R. Fukuda, J. Hasegawa, M. Ishida, T. Nakajima, Y. Honda, O. Kitao, H. Nakai, T. Vreven, K. Throssell, J. A. Montgomery, Jr., J. E. Peralta, F. Ogliaro, M. J. Bearpark, J. J. Heyd, E. N. Brothers, K. N. Kudin, V. N. Staroverov, T. A. Keith, R. Kobayashi, J. Normand, K. Raghavachari, A. P. Rendell, J. C. Burant, S. S. Iyengar, J. Tomasi, M. Cossi, J. M. Millam, M. Klene, C. Adamo, R. Cammi, J. W. Ochterski, R. L. Martin, K. Morokuma, O. Farkas, J. B. Foresman, D. J. Fox, Gaussian 16, Revision C.01, Gaussian, Inc., Wallingford CT, **2016**.
[18] M. Nakajima, E. Fava, S. Loescher, Z. Jiang, M. Rueping, *Angew. Chem.* **2015**, *127*, 8952 – 8954; *Angew. Chem. Int. Ed.* **2015**, *54*, 8828 – 8832.
[19] E. M. Arnett, C. A. Palmer, *J. Am. Chem. Soc.* **1990**, *112*, 1354-1360